The Initial Growth of Disturbances in a Baroclinic Flow

BRIAN F. FARRELL

Center for Earth and Planetary Physics, Harvard University, Cambridge, MA 02138

(Manuscript received 3 September 1981, in final form 5 April 1982)

ABSTRACT

The growth of perturbations in a baroclinic flow is examined as an initial value problem. Although the long time asymptotic behavior is dominated by discrete exponentially growing normal modes when they exist, these do not form a complete set and initial intensification is shown to be dependent on the continuous spectrum. The vertical structure of perturbations emerges as an important influence on initial growth, and physically realistic disturbances are shown to grow to amplitudes where nonlinear effects are important before obtaining normal mode form.

Connection is made with the work of Arnol'd (1965) and Blumen (1968) and the numerical experiments of Simmons and Hoskins (1979). Application of these results to cyclogenesis in geographically fixed areas is suggested and implied constraints on numerical models discussed.

1. Introduction

Since the pioneering work of Charney (1947) and Eady (1949), baroclinic instability has been accepted as a major source of propagating synoptic-scale disturbances in midlatitudes. The success of the theory in predicting approximately the scale, growth and structure of cyclone waves is by now undisputed. Results such as those of Simmons and Hoskins (1978) have extended the theory to the nonlinear regime. Observational studies have shown it to be of primary importance in atmospheric energetics and in maintenance of the observed mean flow.

The application of linear theory to explaining disturbance growth extends over most of the intensification period, although nonlinear effects are important in the mature and decay phases of cyclone life cycles, (Simmons and Hoskins, 1978). As this work is concerned with the initial growth stage, linear theory will be used throughout.

Most models, including those mentioned above, have begun with the assumption of a perturbation of normal mode form or of infinitesimal amplitude so that normal mode structure prevails over the relevant time of the study. The original work of Charney and Eady cast the quasi-geostrophic equations into an eigenvalue problem and extracted only the exponentially growing and presumably negligible companion complex conjugate decaying modes. Suitably generalized to the flow in question, these were used as initial conditions in most subsequent studies. It has long been recognized (Orr, 1907; Case, 1960; Pedlosky, 1979) that the discrete normal modes do not form a complete set in the sense that an arbitrary initial condition cannot be expressed as a sum of discrete normal modes of suitably chosen amplitude. This defect was traced to the neglect of the so-called continuous spectrum of neutral modes. These together with the discrete normal modes do in fact form a complete set for the canonical problems of Eady and Charney, as was shown by Pedlosky (1964) and Burger (1966), respectively.

The careful reader may be troubled at this point by the implication that these singular neutral modes will play a key role in the development, as indeed they shall. Perhaps viscosity no matter how small would change completely the nature of the solutions. While it is true that the Navier-Stokes equations support a complete set of discrete eigenfunctions and the Euler equations require a continuous infinity of singular functions for completeness, yet it appears true that predictions based on the inviscid equations are valid in the limit of vanishing viscosity, even though this is a singular perturbation in the sense of the theory of differential equations. The question is examined in an exchange between Case (1961) and Lin (1961).

All flows discussed in the following will be assumed inviscid.

The method of analysis employed by Pedlosky and Burger is that of Case (1960) in which the Couette problem was cast into initial value form. The result is a combined Fourier-Laplace integral for the space and time evolution of the initial perturbation. The inversion of these integrals is, in general, a formidable task and results were obtained for the asymptotic limit of long time only. This limit revealed not surprisingly that the exponential growing normal mode, where present, dominated the solution. In the Couette flow, where there exist no exponentially

0022-4928/82/081663-24$10.00

growing modes, the contribution of the continuous spectrum was found to decay algebraically with time and the controversy over the order of this decay (Brown and Stewartson, 1980) seems to have been settled in favor of Orr's original result: the streamfunction decays as t^{-2}.

The contribution of the continuous spectrum in baroclinic problems is a matter of some subtlety. In the Eady problem, Pedlosky (1964) found that for wavenumbers for which there were exponentially growing modes, the contribution asymptotically decayed but for the neutral solutions at wavenumbers above the cutoff of exponential instability, the continuous spectrum combined with the neutral waves to give a neutral asymptotic solution. The Charney problem was shown by Burger to have a similar algebraically growing contribution associated with the continuous spectrum at the discrete neutral points and decay elsewhere where exponentially growing discrete normal modes were found.

In order to study the small time limit of the initial value problem in the most transparent manner, a major simplification will be employed: a single wavenumber in the horizontal will be used. This precludes potentially interesting interference effects arising from the Fourier inversion of Case (1960). The perturbation will be assumed to have infinite horizontal extent and a fixed wavenumber. Multiple wavenumbers which would be appropriate to localized perturbations will be only briefly considered.

To explore these ideas, a simple problem for which a closed form solution exists will be examined first.

2. The Couette problem

Taking $u(z)$ as the velocity profile of a plane-parallel inviscid shear flow, confined between horizontal boundaries at $z = 0, 1$ and $\Psi(x, z, t)$ as the perturbation streamfunction, the nondimensional, linearized equation of motion is:

$$\left(\frac{\partial}{\partial t} + u(z)\frac{\partial}{\partial x}\right)\nabla^2\Psi - \frac{\partial^2 u}{\partial z^2}\frac{\partial \Psi}{\partial x} = 0, \qquad (1a)$$

$$\Psi(0) = \Psi(1) = 0. \qquad (1b)$$

The Couette problem results when the velocity is made linearly increasing with z: $u = z$ for which (1a) becomes

$$\left(\frac{\partial}{\partial t} + z\frac{\partial}{\partial z}\right)\nabla^2\Psi = 0. \qquad (2)$$

Solutions are assumed of the form

$$\Psi = \psi(z)e^{ik(x-ct)}. \qquad (3)$$

Substituting in (2):

$$(z - c)\left\{\frac{\partial^2}{\partial z^2} - k^2\right\}\psi = 0. \qquad (4)$$

Eigensolutions of (4) must satisfy

$$\frac{\partial^2\psi}{\partial z^2} - k^2\psi = 0, \qquad (5a)$$

$$\psi(0) = \psi(1) = 0. \qquad (5b)$$

Two linearly independent solutions of (5a) are

$$\psi_1 = \sinh kz,$$

$$\psi_2 = \cosh kz.$$

Of the general solution $\psi = A\sinh kz + B\cosh kz$, (5b) requires

$$B = 0,$$

$$A\sinh k + B\cosh k = 0,$$

which implies $A = B = 0$, so there exists no such solution.

Nevertheless it is seen by inspection that a general solution of (2) has the form for arbitrary $G(x, z)$:

$$\nabla^2\psi = G(x - zt, z). \qquad (6)$$

This problem is an extreme example of the incompleteness of the eigenfunctions, having none at all. Yet it is clear from (6) that the equation is valid for any initial condition.

The resolution of this dilemma proceeds from a closer examination of (4) (Case, 1960). There are in fact two classes of solution: The above sought discrete eigenmodes, which class is empty, and solutions satisfying

$$\left(\frac{\partial^2}{\partial z^2} - k^2\right)G(z, z_0) = \delta(z - z_0). \qquad (7)$$

When the boundary condition (5b) is imposed, it is easily verified that

$$G(z, z_0) = -\frac{\sinh kz_< \sinh k(1 - z_>)}{k\sinh k}, \qquad (8)$$

where

$$z_< = \begin{cases} z & \text{if } z < z_0 \\ z_0 & \text{if } z \geq z_0, \end{cases}$$

$$z_> = \begin{cases} z & \text{if } z > z_0 \\ z_0 & \text{if } z \leq z_0. \end{cases}$$

In this case of linear shear, the simple identification of the continuum normal mode with (8) is completed by setting

$$c = z_0. \qquad (9)$$

Using (3), the solution of (4) for an initial perturbation of wavenumber k, $\Psi_{0,k}(x, z, 0) = \psi_{0,k}(z)e^{ikx}$ is

$$\psi_k(x, z, t) = \int_0^1 G(z, z_0)e^{ik(x-z_0t)} \times \left\{\left(\frac{\partial^2}{\partial z_0^2} - k^2\right)\psi_{0,k}(z_0)\right\}dz_0\,, \quad (10)$$

which may be verified by substitution.

Using (9), (10) can be written as an integral over the normal modes:

$$\psi_k(x, z, t) = \int_0^1 G(z, c)e^{ik(x-ct)} \times \left\{\left(\frac{\partial^2}{\partial c^2} - k^2\right)\psi_{0,k}(c)\right\}dc. \quad (11)$$

For a fixed eigenvalue c, $G(z, c)$ may be interpreted as the eigenfunction and $\{(\partial^2/\partial z_0^2 - k^2)\psi_0(z_0)\}_{z_0=c}$ as the corresponding amplitude.

Assuming $\psi_{0,k}(z) = c \sin m\pi z \cos kx$, the term in curly brackets in (10) becomes $-c[(m\pi)^2 + k^2] \sin m\pi z \cos kx$. Substituting this and (8) in (10), repeated integration by parts and taking the real part produces the closed form solution (Orr, 1907):

$$\psi(x, z, t) = \frac{c(k^2 + (m\pi)^2)}{2k \sinh k}\left\{\begin{array}{l}\{\sinh k \cos[kx + (m\pi - kt)z] - \sinh k(1 - z) \cos kx \\ \quad - \sinh kz \cos[kx + (m\pi - kt)]\}/[k^2 + (m\pi - kt)^2] \\ \quad - \{\sinh k \cos[kx - (m\pi + kt)z] - \sinh k(1 - z) \cos kx \\ \quad - \sinh kz \cos[kx - (m\pi + kt)]\}/[k^2 + (m\pi + kt)^2]\end{array}\right\}. \quad (12)$$

The long time asymptotic behavior of the stream function is $O(t^{-2})$ but the appearance of the term $[k^2 + (m\pi - kt)^2]$ in the denominator suggests that for some time after an initial perturbation the disturbance may grow.

It is important to note a possible difficulty in interpreting the nonexponential growth of perturbations. If the amplitude of the initial perturbation in this linear problem is held fixed as the vertical wavenumber is increased, in an attempt to explore the initial value problem dynamics, an ambiguity arises because the energy per unit length in x, given by

$$E = \frac{k}{4\pi}\int_0^{2\pi/k}\int_0^1 (\psi_x^2 + \psi_z^2)dxdz, \quad (13)$$

increases with m. Although in problems of interest in meteorology the streamfunction itself represents a pressure perturbation, the constancy of which may have physical justification as vertical wavenumber is changed, most results below are displayed in terms of perturbation total energy normalized by the initial total energy, which shows the growth of perturbations in the most easily interpreted form.

The total energy (13) may be evaluated approximately both for $t = 0$ and for the approximate time of the maximum of (12), $t_m = m\pi/k$:

$$E(0) = \frac{c^2(k^2 + (m\pi)^2)}{8k^2},$$

$$E(t_m) \simeq \frac{c^2[k^2 + (m\pi)^2]^2}{16k^4} \times \left\{1 - \frac{4(m\pi)^2}{k^2 + (2m\pi)^2}\frac{\tanh k/2}{k/2}\right\}.$$

The ratio

$$\frac{E(t_m)}{E(0)} = \frac{[k^2 + (m\pi)^2]}{2k^2} \times \left\{1 - \frac{4(m\pi)^2}{[k^2 + (m\pi)^2]}\frac{\tanh k/2}{k/2}\right\} \quad (14)$$

is plotted as a function of k and $m\pi$ in Fig. 1a. Note that although the plot is continuous for clarity of presentation, only integer values of m satisfy the boundary condition (1b). The maximum energy occurs for longest horizontal and shortest vertical scale. An estimate of growth rate is made by dividing the maximum of energy by the time it occurs after the initial perturbation $t_m = m\pi/k$; the result is plotted in Fig. 1b. The maximum growth rate occurs for $k \approx 3.0$, suggesting a scale selection for "burst" generation in exponentially stable flows, when the relevant mechanism is extraction of mean flow energy by perturbations of stochastic origin.

The evolution of the streamfunction is calculated from (12) for $k = 3.0$ and $m = 6$ and the magnitude shown as a function of time in Fig. 2a, b. Also shown (Fig. 2c) is the exact normalized energy as a function of time, calculated from (12) and (13) and the effective growth rate $2kc_{i_{\text{eff}}} = 1/EdE/dt$ (Fig. 2d).

There appear to be three stages in this growth: a relatively quiescent period immediately following the perturbation, a period of rapid growth and a period of rapid decay to the asymptotic phase where the perturbation decays as t^{-2}. Only this last stage is addressed in traditional asymptotic treatments.

Note that the rapid growth of the perturbation is coincident with a decrease in the vertical wavenum-

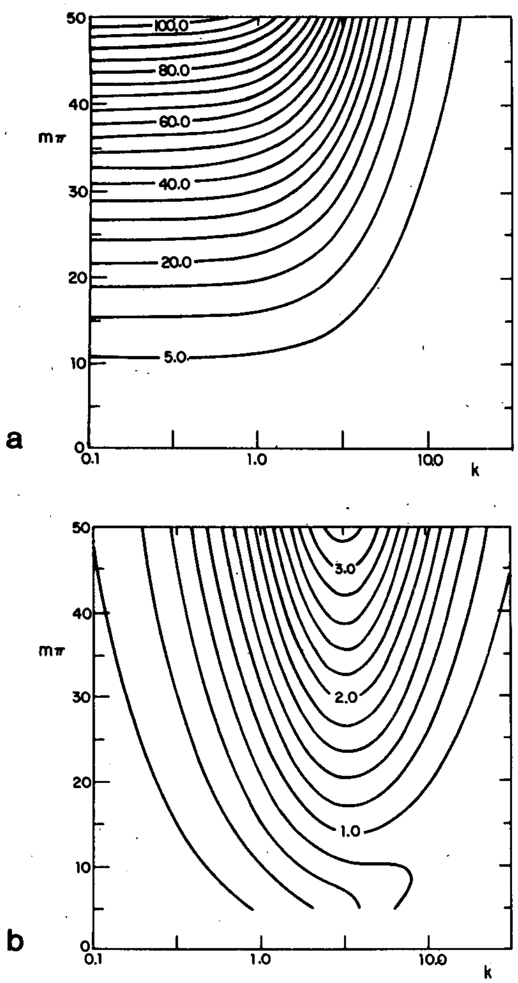

FIG. 1. (a) Approximate maximum normalized kinetic energy for the Couette problem as a function of perturbation horizontal wavenumber k and vertical wavenumber $m\pi$. (b) As in (a) but for approximate growth rate of perturbations.

ber, a phenomena that will be referred to in the following analysis.

3. Discussion of the Couette problem

As an example of the initial growth of perturbations, the Couette problem is particularly attractive because it is by far the simplest and displays much of the relevant physics. With this solution as an analogy, the results to be obtained for baroclinic flows will be introduced and some preliminary comments made.

We note first that even when linear perturbation theory predicts no instability, it cannot be concluded that the flow is stable. If neutral solutions exist, then stability can only be ascertained by examining higher-order terms in the perturbation expansion. Even when we are fortunate enough, as in the above example, to be in possession of a complete set of modes (for the linear problem) whose integral contribution eventually decays, the amplitude of disturbance for which higher-order terms may lead to instability is, in general, unknown. In fact the observation of small-scale inflection points appearing to destabilize an otherwise stable flow in experiments (Landahl, 1975) is interesting in this regard. These observations make the fact that substantial increases in amplitude result from linear theory especially important.

In geophysical application it is often the case that modest increases in amplitude suffice to explain an observed phenomenon. For example, a 1 mb initial perturbation in the geostrophic streamfunction growing by an order of magnitude to 10 mb would be a significant deepening.

The equations describing baroclinic and barotropic waves are very similar to those which we have examined. Although the interpretation of terms is different, a parallel phenomenon is seen and even when exponentially growing modes are present, the initial growth can dominate the solution over relevant time scales, that is; the normal mode structure develops only after significant growth has occurred by this alternate mechanism.

Returning to the example of parallel flow of an inviscid fluid, an energy integral may be obtained in the standard way:

$$\frac{d}{dt}\int_0^1 \frac{1}{2}(\overline{\psi_x^2}+\overline{\psi_z^2})dz = \int_0^1 U_z\overline{\psi_x\psi_z}dz, \qquad (15)$$

where

$$\overline{(\ldots)} = \lim_{x\to\infty}\int_{-x}^{x}(\quad)dx.$$

This relates the increase in disturbance energy to the work done on the perturbations by the Reynolds stress. Parallel expressions exist for baroclinic and barotropic flows (Pedlosky, 1979). While no normal modes exist for which the relative phase of the vertical and horizontal velocity is such as to render the right-hand side of (15) positive, an initial perturbation may have this property or as happened in the above may acquire it by virtue of being sheared by the basic state flow. (Incidently, this explains the slow initial phase growth in the above solution (Fig. 2d); ψ_x and ψ_z are initially in quadrature.) This phenomenon is familiar to students of meteorology from the work of Pedlosky (1970), whose small amplitude waves continue to grow through a large part of the vacillation cycle, after the nonlinear terms have stabilized the flow to normal mode perturbations. This occurs because the disturbances are still in possession of relative phases which result in their extracting energy from the mean flow. If, by a conspiracy of intent, the initial condition were of this form, the same solution would of course be found even though the flow was not initially unstable.

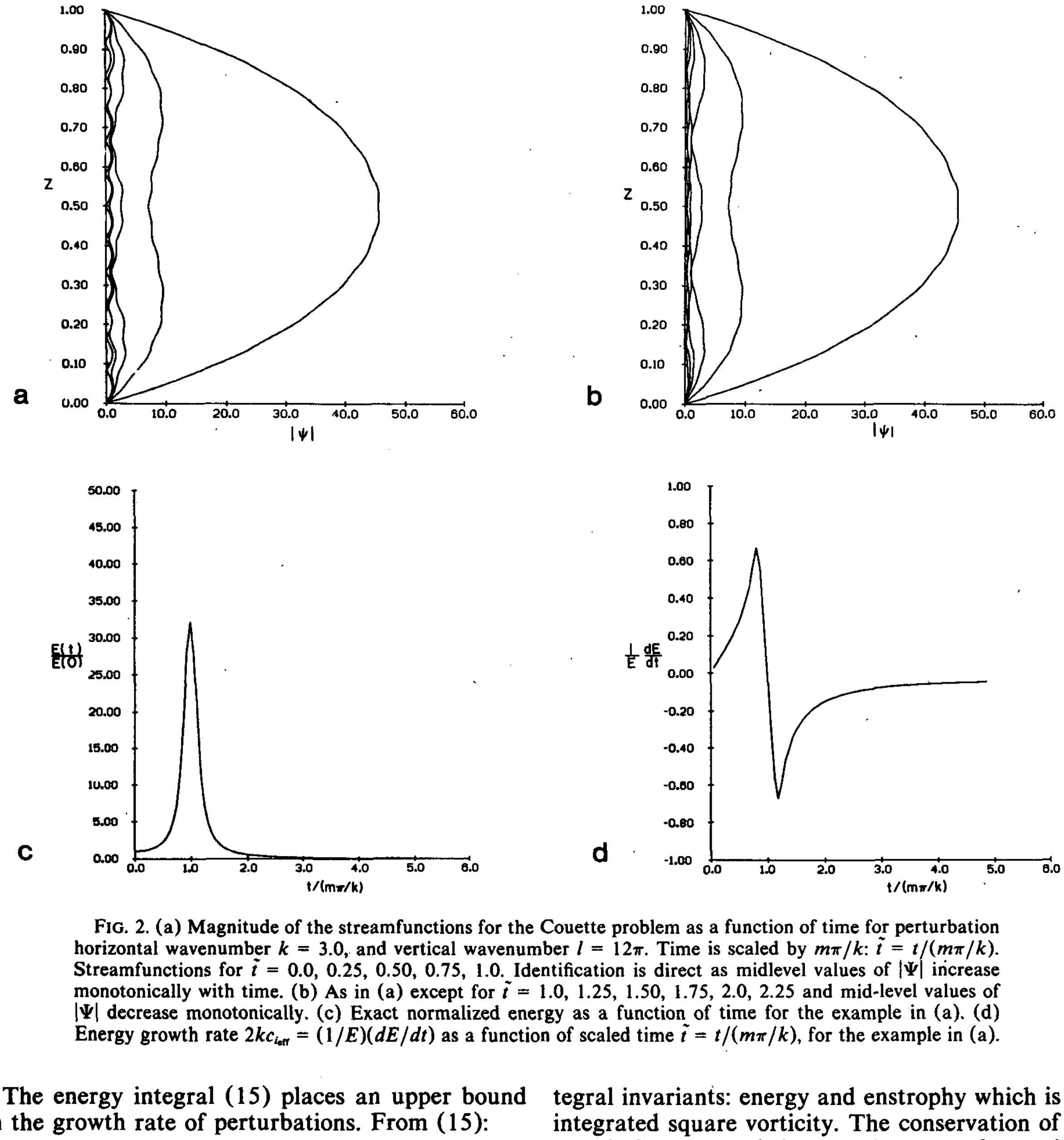

FIG. 2. (a) Magnitude of the streamfunctions for the Couette problem as a function of time for perturbation horizontal wavenumber $k = 3.0$, and vertical wavenumber $l = 12\pi$. Time is scaled by $m\pi/k$: $\tilde{t} = t/(m\pi/k)$. Streamfunctions for $\tilde{t} = 0.0, 0.25, 0.50, 0.75, 1.0$. Identification is direct as midlevel values of $|\Psi|$ increase monotonically with time. (b) As in (a) except for $\tilde{t} = 1.0, 1.25, 1.50, 1.75, 2.0, 2.25$ and mid-level values of $|\Psi|$ decrease monotonically. (c) Exact normalized energy as a function of time for the example in (a). (d) Energy growth rate $2kc_{i_{eff}} = (1/E)(dE/dt)$ as a function of scaled time $\tilde{t} = t/(m\pi/k)$, for the example in (a).

The energy integral (15) places an upper bound on the growth rate of perturbations. From (15):

$$\frac{dE}{dt} = \frac{d}{dt}\int_0^1 \frac{1}{2}(\overline{\psi_x^2} + \overline{\psi_z^2})dz \leqslant |U_z|_{\max}\int_0^1 |\bar{\psi}_x||\bar{\psi}_z|dz,$$

which together with the inequality

$$\bar{\psi}_x^2 + \bar{\psi}_z^2 \geqslant 2|\bar{\psi}_x||\bar{\psi}_z|$$

gives

$$\frac{1}{E}\frac{dE}{dt} \leqslant |U_z|_{\max}.$$

The example in Fig. 2d obtains ~70% of this maximum.

The inviscid incompressible Navier-Stokes equations in two dimensions possess two independent integral invariants: energy and enstrophy which is the integrated square vorticity. The conservation of energy is familiar and the equations are often written to explicitly display the conservation of vorticity. Vorticity is conserved point by point, so any other function of vorticity when integrated over the domain of flow, is also a conserved quantity but is not an independent invariant. In the case of quasi-geostrophic flow, the energy and pseudopotential vorticity are the parallel conserved quantities (Charney, 1973). The reader is cautioned that these quantities are conserved by the complete equations; however, the linearized equations can be closed by including the second-order corrections to the mean flow (Pedlosky, 1979). If the evolution of an initial disturbance is viewed as the trajectory of a point in a suitably defined phase space, then the integral invariants limit

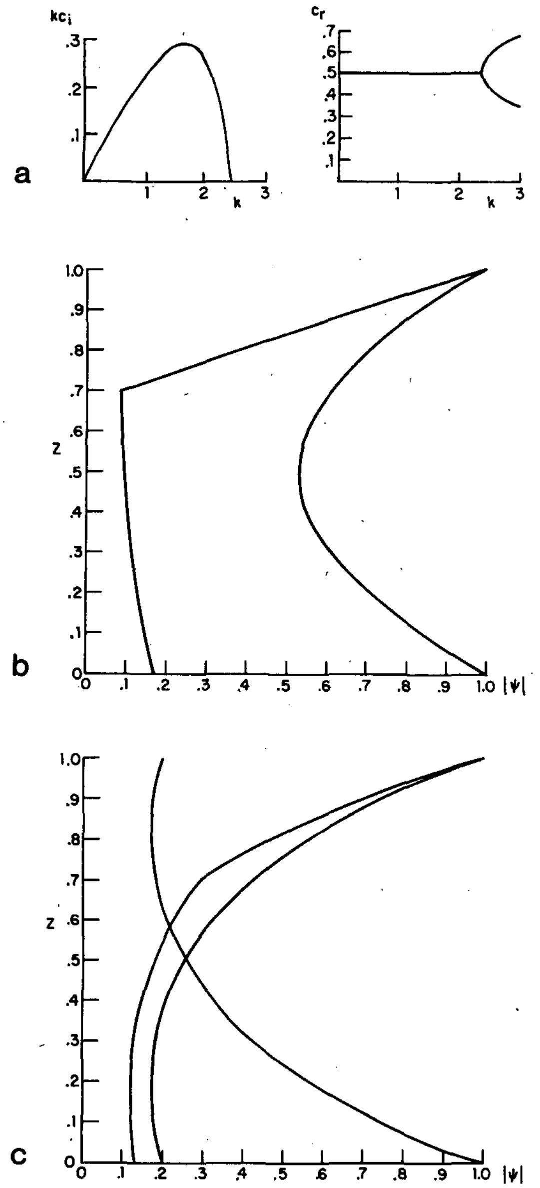

FIG. 3. (a) Phase speed c_R and growth rate kc_i for the discrete normal modes in the Eady problem. There is also a complex conjugate decaying mode for $0 < k < 2.3994$. (b) Normal mode streamfunction amplitude at horizontal wavenumber $k_m = 1.6062$ for the Eady problem. An example of the continuum normal modes at $c = 0.7$ is shown. (c) As in (b) except for $k = 3.0$ in the neutral region.

this trajectory to surfaces which satisfy energy and vorticity conservation. These constraints potentially limit the extent to which a perturbation to a basic state may grow. For the case of stationary, plane, curvilinear, inviscid and incompressible flows the following can be shown by integral techniques to hold for small perturbations (Arnol'd, 1965):

$$\frac{d}{dt}\int (\nabla\psi)^2 + \frac{\nabla\Psi}{\nabla\Delta\Psi}(\Delta\psi)^2 dxdz = 0, \qquad (16)$$

where $\psi = \psi(x, z, t)$ = perturbation streamfunction, and $\Psi = \Psi(z)$ = streamfunction of the basic state.

The ratio appearing in (16) is well defined, because stationary requires $\nabla\Psi$ and $\nabla\Delta\Psi$ be parallel.

In our examples, $\nabla\Psi/\nabla\Delta\Psi = U(z)/U''(z)$, so that (16) may be written

$$\frac{d}{dt}\int (\nabla\psi)^2 + \frac{U}{U''}(\Delta\psi)^2 dxdz = 0. \qquad (17)$$

The Rayleigh and Fjortoft theorems (Charney, 1973) are immediate consequences of (16), because a change in sign of

$$F(z) = \frac{U}{U''}, \qquad (18)$$

in the domain of flow may allow arbitrary growth. In fact, this integral constraint extends these results as shown by the examples in Arnol'd (1965).

Concentrating on the case of stable flows with $U/U'' > 0$ it can be seen that (17) permits the energy of the perturbation to grow at the expense of the enstrophy. Furthermore, the extent to which a change in enstrophy is able to be traded for increased energy is governed by the term U/U''.

For these problems, the stability is not affected by the addition of a uniform velocity to the basic state, U. The choice resulting in the tightest bound from (17) is preferred. For instance, Fjortoft's theorem results when $U = 0$ is coincident with the inflection point $U'' = 0$.

As an example, the basic state

$$U(z) = z + \frac{\epsilon z^2}{2},$$

gives for (18):

$$F(z) = \frac{z + (\epsilon z^2/2)}{\epsilon}, \qquad (19)$$

which for $\epsilon \to 0$ allows arbitrary large increases in energy for a decrease in enstrophy. Note that this limit corresponds to the Couette problem. Indeed it is easily verified by inspection of (2) that, despite the change in vertical wavenumber and energy entailed in the examples above, the enstrophy remains constant. If $F(z)$ is viewed as an indication of the potential of a basic state to exhibit initial value growth, then the Couette problem at first glance appears to have unlimited potential. For other basic states the bound is tighter, as can be seen by allowing ϵ large in (19). The Couette problem is exceptional in the sense that while (16) fails to provide a tight bound on the growth of perturbations, a much better bound can be obtained (Appendix A).

Of course, there is no guarantee that the detailed dynamics of a perturbation will give rise to a decrease in enstrophy and concomitant increase in energy, but this is usually observed for high enstrophy initial conditions.

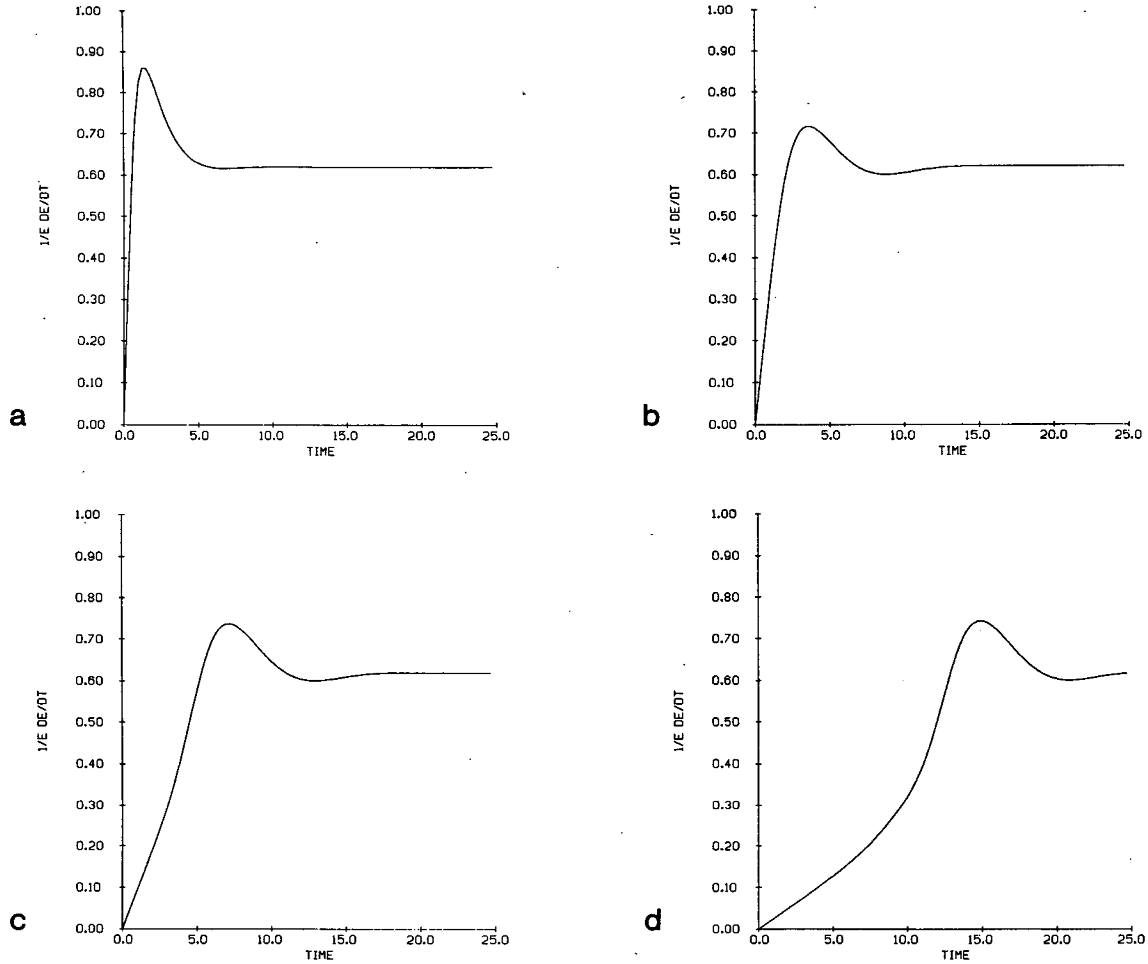

FIG. 4. The energy growth rate $2kc_{i_{\rm eff}} = (1/E)(dE/dt)$ for the Eady problem with horizontal wavenumber $k_m = 1.6062$ and initial perturbation vertical wavenumber $l = m\pi$, with $m = 0, 2, 4, 8$, in (a), (b), (c) and (d), respectively.

If the vertical wavenumber is large, there is potential for great energy growth even for modest values of $F(z)$, as can be seen by noting that the ratio of enstrophy to energy for $\psi(z) \approx \sin mz$ is:

$$(\Delta\psi)^2/(\nabla\psi)^2 \approx m^2.$$

Although (16) gives no bound in the case of unstable flows for which $F(z)$ changes sign in the domain, the initial value growth mechanism continues to operate, as will be shown by examples to follow. In fact, low vertical wavenumber normal modes, whether neutral or unstable, appear to be efficiently produced by this mechanism, resulting in initial growth rates much higher than would be expected from an examination of their eigenvalues. It is important to note in this connection that these discrete and continuous normal modes have no orthogonality properties, so that no result of the kind expressed in Parseval's theorem (Jeffreys and Jeffreys, 1956) exists. Because of this, it is possible for a high amplitude discrete normal mode to be present in the expansion of a small initial perturbation, only to be revealed when the continuous spectrum decays away.

4. Baroclinic initial value problems

The behavior of small perturbations to a baroclinic fluid in zonal flow is governed by the linearized equation expressing the conservation of pseudo-potential vorticity (Pedlosky, 1979):

$$\left(\frac{\partial}{\partial t} + U\frac{\partial}{\partial x}\right)q + \frac{\partial\psi}{\partial x}\frac{\partial\Pi}{\partial y} = 0, \qquad (20a)$$

with a boundary condition requiring the vertical velocity to vanish on rigid horizontal surfaces:

$$\left(\frac{\partial}{\partial t} + U\frac{\partial}{\partial x}\right)\frac{\partial\psi}{\partial z} - \frac{\partial U}{\partial z}\frac{\partial\psi}{\partial x} = 0, \quad z = 0, z_T, \qquad (20b)$$

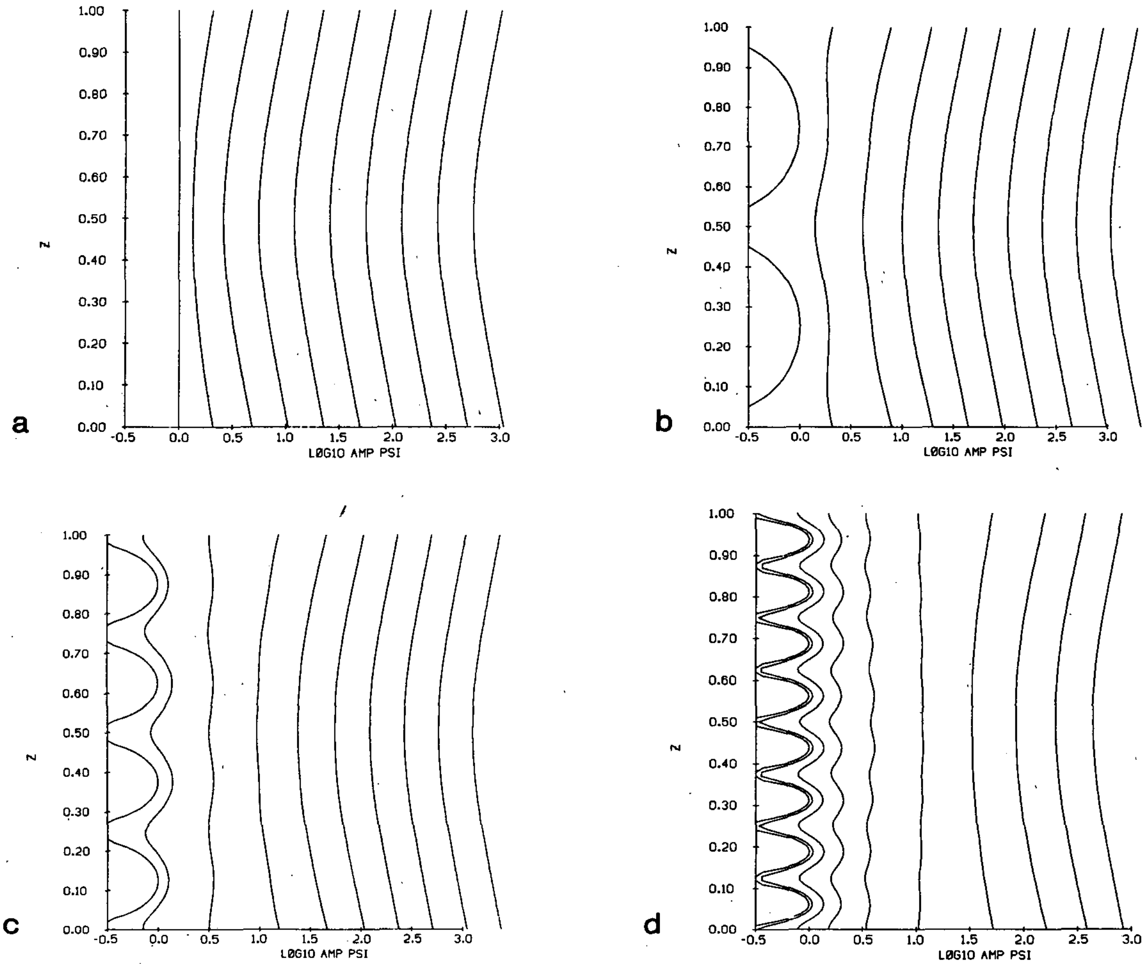

FIG. 5. Streamfunction amplitude for the examples in Fig. 4, as a function of height z. Samples are taken at $t = N\Delta t$, $N = 0, 1, 2 \cdots 9$, $\Delta t = 2.5$. Identification is direct as surface values of $|\Psi|$ increase monotonically with time.

where:

- x eastward coordinate
- y northward coordinate
- z height
- $U(z)$ basic state zonal velocity
- ψ perturbation geostrophic streamfunction
- q $\nabla^2\psi + (1/\rho\epsilon)(\partial/\partial z)[\epsilon\rho(\partial\psi/\partial z)]$ (perturbation potential vorticity)
- ϵ f^2/N^2 (square ratio of the Coriolis parameter to the Brunt-Väisälä frequency)
- ρ density
- Π_y $\beta - (\partial^2 U/\partial y^2) - (1/\rho\epsilon_s)(\partial/\partial z)[\epsilon\rho_s(\partial U/\partial z)]$ (meridional gradient of potential vorticity of the basic state)
- β $\partial f/\partial y$.

Notice that (20) is made to correspond to (1) except for the boundary condition

$$\psi_z(0) = \psi_z(z_T) = 0,$$

by considering the boundary as a δ-function in π_y (Bretherton, 1966; Lindzen *et al.*, 1980); this is accomplished by bending the velocity profile $U(z)$ in the immediate vicinity of the boundary so that $U_z = 0$, $z = 0$, z_T.

The energy integral for the y-independent perturbations is

$$\frac{dE}{dt} = \frac{d}{dt}\int_0^{z_T} \frac{\rho}{2}[\overline{(\psi_x)^2} + \epsilon\overline{(\psi_z)^2}]dz$$

$$= \int_0^{z_T} \rho\epsilon \frac{\partial U}{\partial z}\overline{\frac{\partial\psi}{\partial x}\frac{\partial\psi}{\partial z}}dz. \qquad (21)$$

Comparing this with (15), the structure of the equation is the same but the terms on the left-hand side are interpreted as kinetic and potential energy, respectively, while the source on the RHS is heat flux down the global temperature gradient. It is expected that an initial perturbation which results in

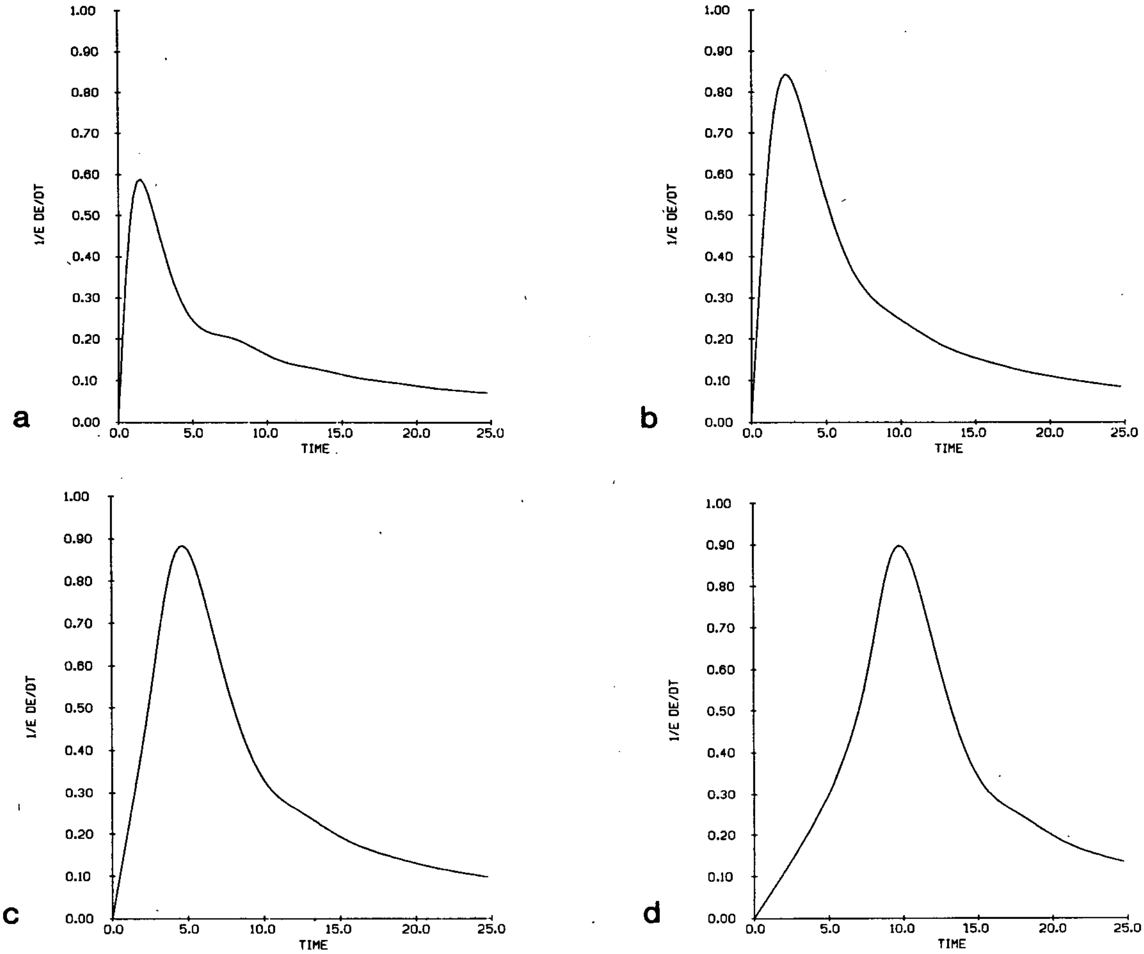

FIG. 6. As in Fig. 4, except for k = 2.4.

the RHS of (21) being positive or which obtains this correlation under the action of the basic-state shear will exhibit initial growth.

The energy integral (21) places an upper bound on the growth rate of perturbations in parallel with that derived in Section 3 for the inviscid shear flow:

$$\frac{1}{E}\frac{dE}{dt} \leqslant |\sqrt{\epsilon}U_z|_{\max}\,.$$

This bound is approached in examples to follow.

The result of Arnol'd has been generalized to quasi-geostrophic flows (Blumen, 1968). The twin constraints of energy and potential vorticity conservation require that perturbation energy and enstrophy be related as the disturbance evolves by

$$\frac{d}{dt}\left\{\int_0^{z_T}\rho(\overline{\psi_x^2}+\epsilon\overline{\psi_z^2}) - \frac{U(z)}{\beta-\dfrac{1}{\rho\epsilon}\dfrac{\partial}{\partial z}\left(\rho\epsilon\dfrac{\partial U}{\partial z}\right)}\overline{q^2}dz\right\} = 0, \quad (22)$$

where the boundary terms have been absorbed by bending $U(z)$ so $U_z = 0$ at the boundaries and the β-plane approximation has been made.

The criterion for stability:

$$F(z) = -U(z)\Bigg/\left[\beta - \frac{1}{\rho\epsilon}\frac{\partial}{\partial z}\left(\rho\epsilon\frac{\partial U}{\partial z}\right)\right] > 0,$$

implies for an exponentially stratified atmosphere that $\rho = \rho_0 e^{-z/H}$, with ϵ constant so that

$$-U(z)\Bigg/\left(\beta + \frac{U_z}{H} - U_{zz}\right) > 0.$$

The fluid is stable if $\beta + (U_z/H) - U_{zz}$ is of one sign, in which case a frame of reference velocity exists for which $F(z) > 0$ and the initial growth mechanism would allow the energy of perturbations to grow as described above; whether the potential growth is realized would have to be determined by solving (20) for any particular initial condition.

The above criterion has been exploited to produce a flow stabilized to exponentially growing distur-

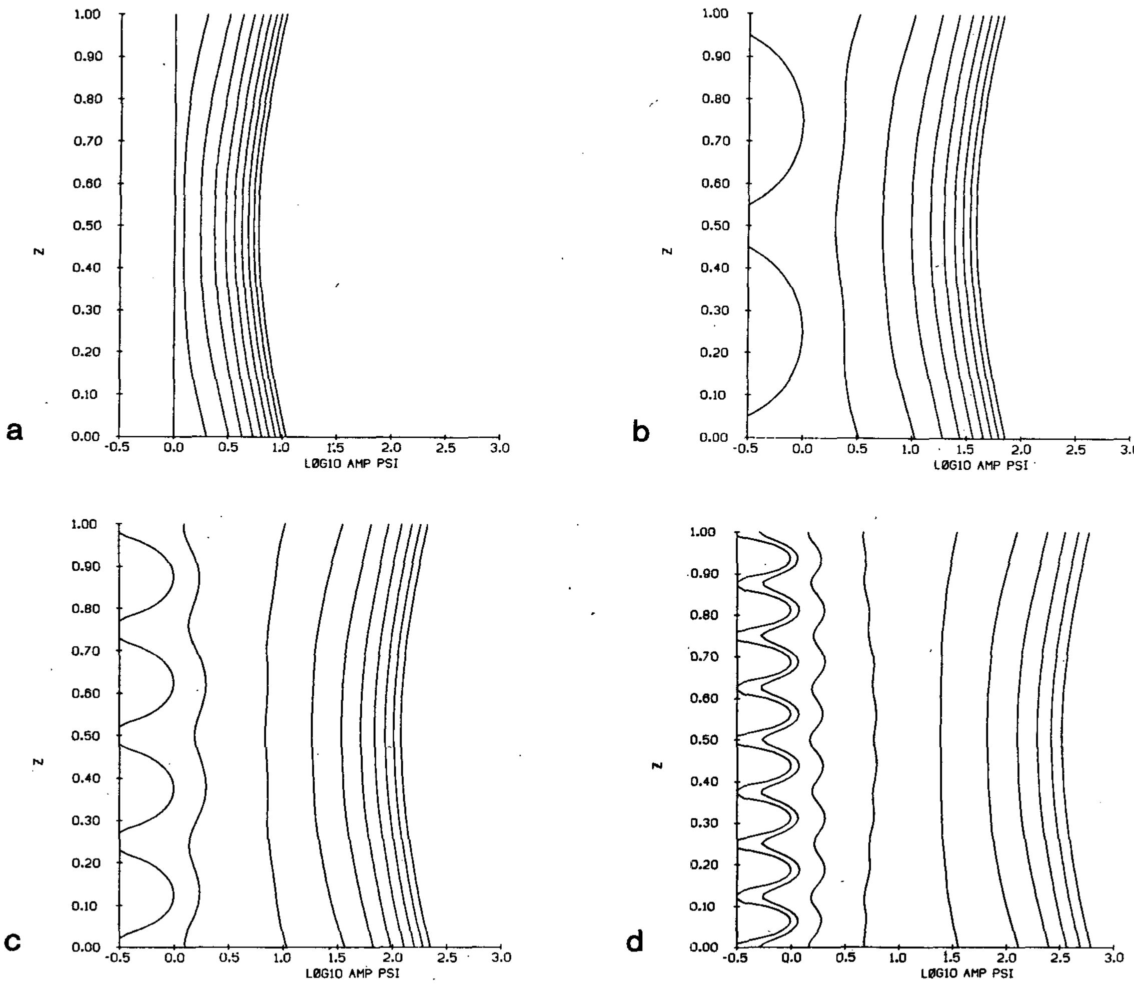

FIG. 7. As in Fig. 4, except for $k = 2.4$.

bances by modifying $U(z)$ (Lindzen *et al.*, 1980):

$$\Pi_y = \beta + \frac{U_z}{H} - U_{zz} \geq 0 \quad 0 \leq z \leq z_T .$$

The response of such a flow to an initial disturbance is examined in Section 9.

In summary, we will show that baroclinic flows can exhibit non-normal mode growth of an initial perturbation whether the flow supports exponentially growing normal modes or not.

5. Preliminary discussion of baroclinic initial value examples

The canonical examples of baroclinic instability for the quasi-geostrophic equations are the solutions of Charney (1947) and Eady (1949). These have been shown to possess a complete set of normal modes when the discrete normal modes (there are two for every horizontal wavenumber except for isolated neutral points in the Charney problem) are augmented by the continuum of neutral modes (Pedlosky, 1964, Burger, 1966). The solution is found in terms of a Laplace transform of the relevant Green functions in the manner of Case (1960), who used this formalism for the Couette problem. The initial value problem is solved by inversion of these transforms. Unfortunately, the Greens functions, while simply expressed in terms of the solutions of the equation, result in cumbersome Laplace inversions. Initial value results were confined, in the above-mentioned investigations, to the long time asymptotics which show the familiar discrete normal mode spectra and decay of the continuum contribution. The exception was the Eady neutral waves where a component of the continuous spectrum combines with the neutral discrete normal modes to produce an O(1) asymptotic contribution and the isolated neutral points of the Charney problem where the continuum contribution grows by $O(t)$.

The initial growth of perturbations could, in principle, be found by inverting numerically the Laplace

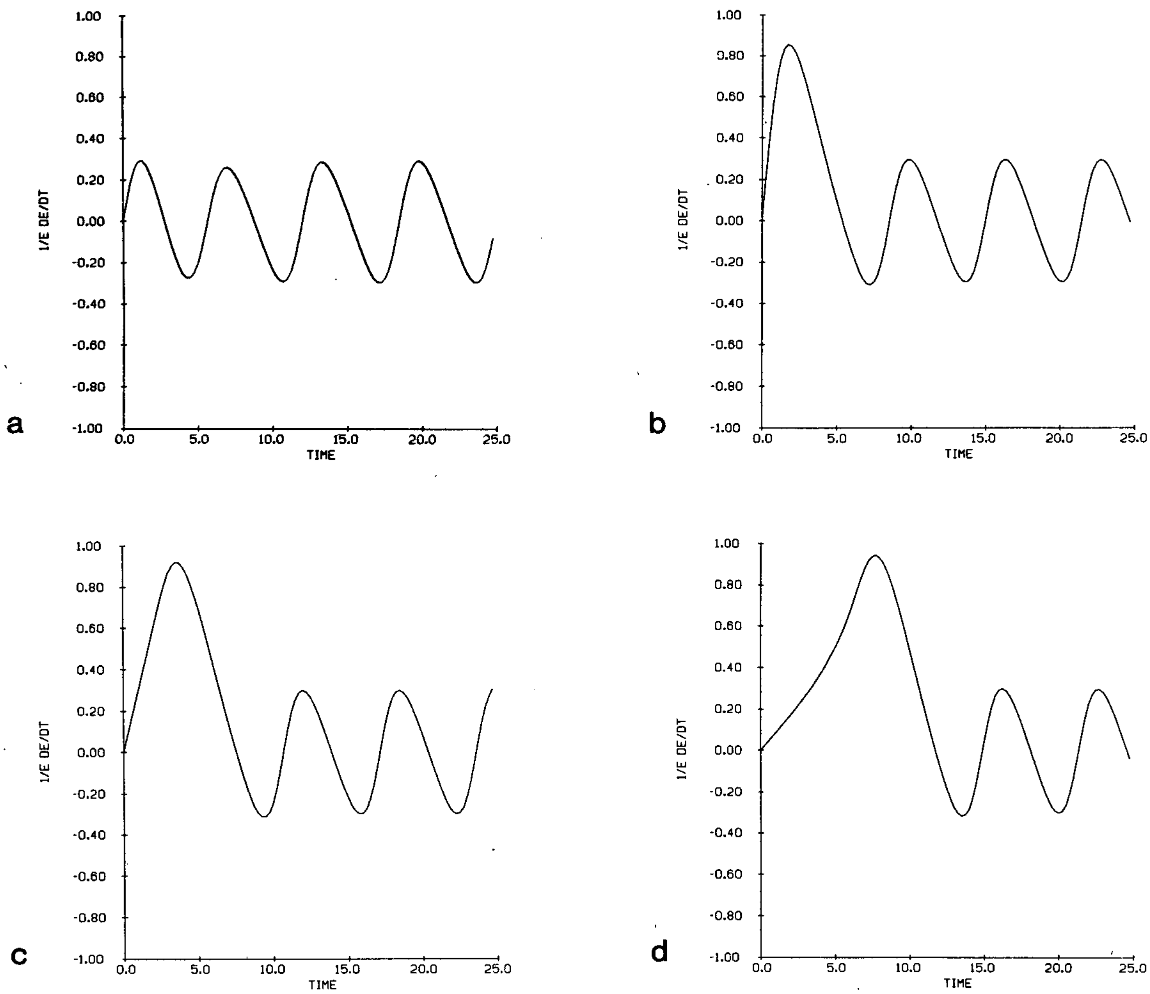

FIG. 8. As in Fig. 4, except for $k = 3.0$.

transform but this approach presents many difficulties. Instead, the results to be presented below were derived by integrating the equations for different initial conditions. The method employed (Appendix B) was to assume normal mode solutions:

$$\psi_N(x, z, t) = \psi_N(z)e^{ik(x-c_Nt)}, \tag{23}$$

and finite difference (20) in z. The resulting matrix was then resolved into normal modes ψ_N, using the highly efficient QR algorithm (Wilkinson, 1965).

An initial perturbation can be projected on these normal modes and the streamfunction $\theta(x, z, t)$ at later time found by summing over (23):

$$\theta(x, z, t) = \sum_N a_N\psi_N(z)e^{ik(x-c_Nt)} \tag{24}$$

where

$\psi_N(z)$ Nth normal mode
c_N complex phase speed of Nth normal mode
a_N projection of initial condition on $\psi_N(z)$.

The advantage of this method is that once the eigenvectors and eigenvalues have been extracted for a given horizontal wavenumber k, the integration for various initial conditions requires little computational effort. In addition, the projection of the initial condition on the discrete normal modes immediately reveals to what extent they are excited. The fact that the complete set of normal modes are independent but not orthogonal, allows the amplitude of initial excitation of exponentially growing modes to be large for a relatively modest initial disturbance.

The disadvantage of this method is that it requires the approximation of the continuum spectrum by a finite number of modes, or equivalently, the approximation of the continuous atmosphere by a finite number of levels (Pedlosky, 1979). Experience shows that accurate solutions for vertical wavenumber-4 perturbations require no more than 50 levels, although as many as 150 levels have been used to check accuracy.

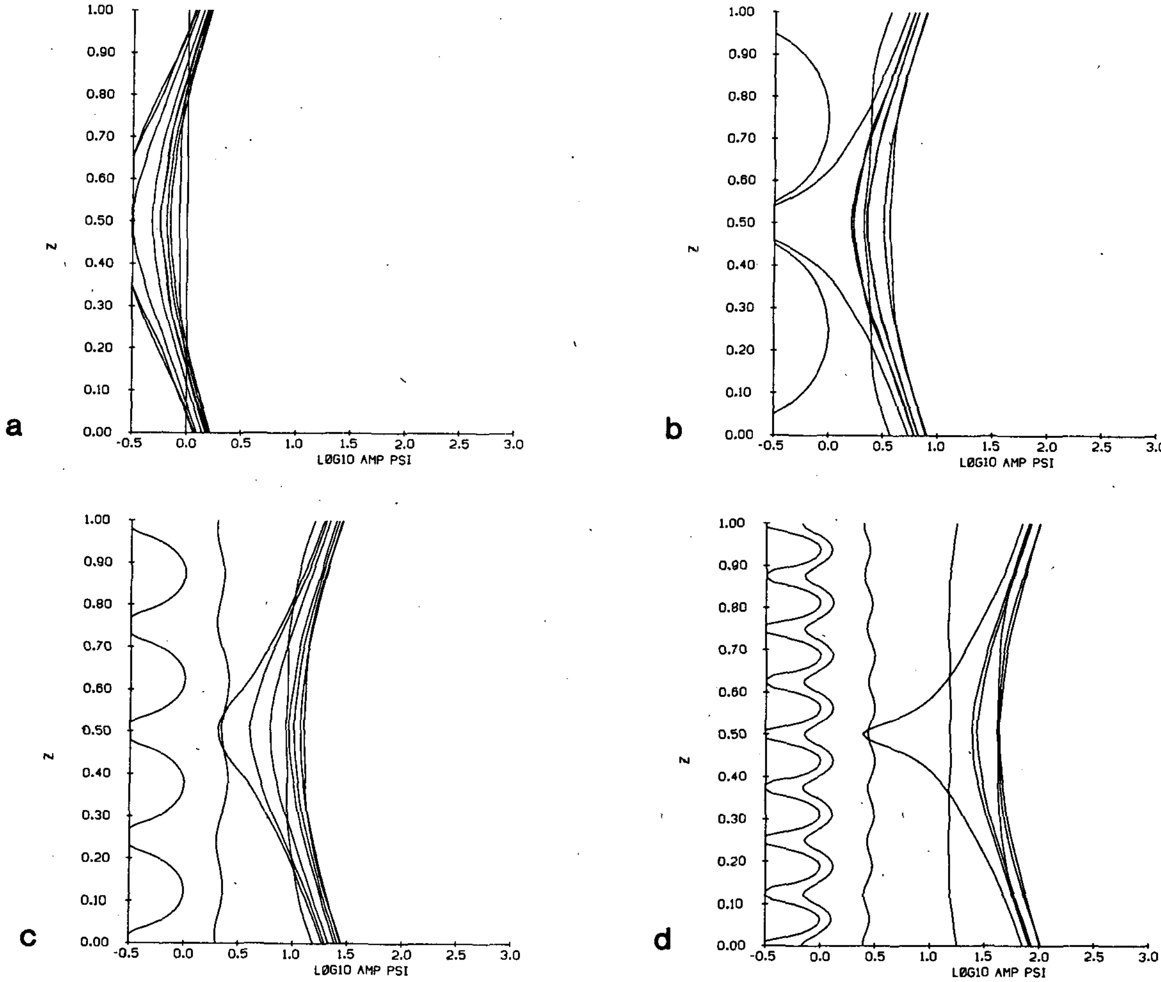

FIG. 9. As in Fig. 4, except for $k = 3.0$.

6. The Eady problem

The Eady problem results when (20) is restricted to $\beta = 0$, N constant, the Boussinesq approximation is made, the shear assumed linear [$U(z) = \Lambda z$], and horizontal boundaries are imposed at $z = 0, 1$:

$$(\tilde{z} - \tilde{c})\left(\frac{\partial^2\psi}{\partial\tilde{z}^2} - \tilde{k}^2\psi\right) = 0, \quad (25a)$$

$$(\tilde{z} - \tilde{c})\psi_{\tilde{z}} - \psi = 0, \quad \tilde{z} = 0, 1, \quad (25b)$$

where solutions for infinite meridional scale of the form $\psi(x, z, t) = \psi(z)e^{ik(x-ct)}$, have been assumed and the following nondimensionalization made:

- $\tilde{k}$ $kH/\sqrt{\epsilon}$ (nondimensional horizontal wavenumber)
- $\tilde{z}$ z/H (nondimensional height)
- $\tilde{t}$ $t\Lambda\sqrt{\epsilon}$ (nondimensional time)
- H scale height
- ϵ f^2/N^2
- f Coriolis parameter
- N Brunt-Väisälä frequency
- Λ $\partial U/\partial z$ (shear of mean flow, assumed constant).

For reference we note that typical midlatitude values of constants

- β 1.6×10^{-11} s^{-1} m^{-1}
- H 8×10^3 m
- f 10^{-4} s^{-1}
- N 10^{-2} s^{-1}
- Λ 1.25×10^{-3} s^{-1},

so that $\tilde{k}$ is related to dimensional wavelength by

$$\lambda = \frac{H}{\sqrt{\epsilon}}\frac{2\pi}{\tilde{k}} = \frac{5 \times 10^6 \text{ m}}{\tilde{k}} \quad (26)$$

and $\tilde{t}$ is related to dimensional time by

$$t = \frac{\tilde{t}}{\Lambda\sqrt{\epsilon}} = 22\tilde{t}\ \text{h}. \quad (27)$$

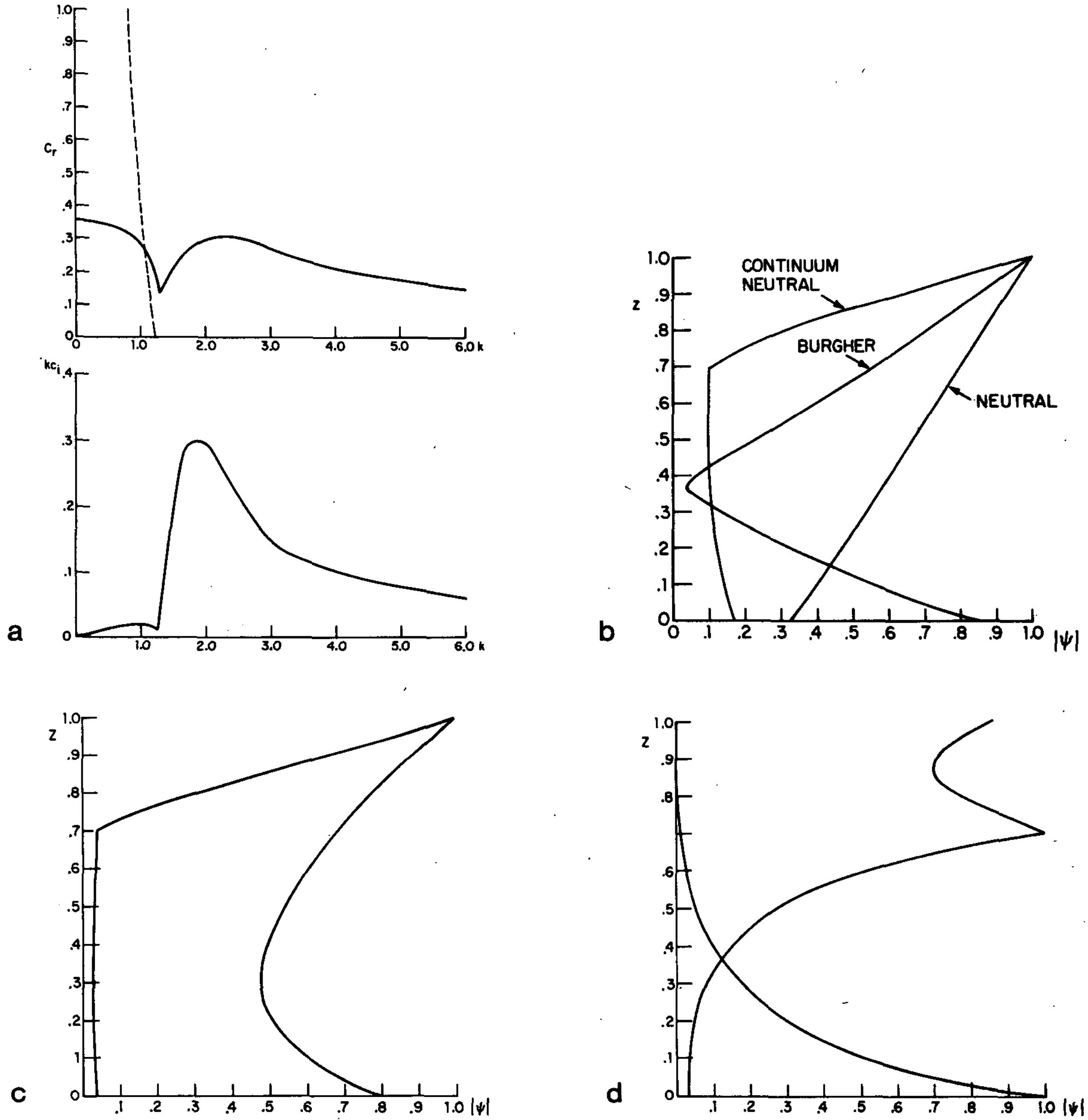

FIG. 10. (a) Phase speed c_r and growth rate kc_i for the discrete normal modes in the Green problem. There are also complex conjugate decaying modes. The (negative) phase speed of the retrograde neutral mode is indicated by a dashed line. (b) Normal mode streamfunction amplitude at $k_m = 1.0$, together with the continuum normal mode at $c = 0.7$. (c) As in (b) except for $k = 1.8$. (d) As in (b) except for $k = 6.0$.

It is important to note in evaluating quantities which are functions of $\tilde{t}$ that a unit of nondimensional time is related to dimensional time by the inverse shear. Here we have assumed a 10 m s^{-1} zonal velocity at 8 km resulting in a 22 h $\tilde{t}$, but three- or even four-times this velocity may be appropriate to strong jets resulting in a 6–8 h $\tilde{t}$.

Tildes will be dropped in the following.

The eigenvalues of the discrete normal modes are shown in Fig. 3a. There are two such modes at each value of the horizontal wavenumber k. For $0 < k < 2.39994$ these correspond to complex conjugate modes, one growing and one decaying; for $k > 2.3994$ there are two neutral waves. The maximum growth rate occurs for $k_m = 1.6062$. Normal mode structure at k_m is shown in Fig. 3b along with an example of the continuous spectrum at $c = 0.7$. Fig. 3c shows the normal mode structure at $k = 3.0$, in the region of neutral discrete normal modes.

Because the long time asymptotic limit of an ex-

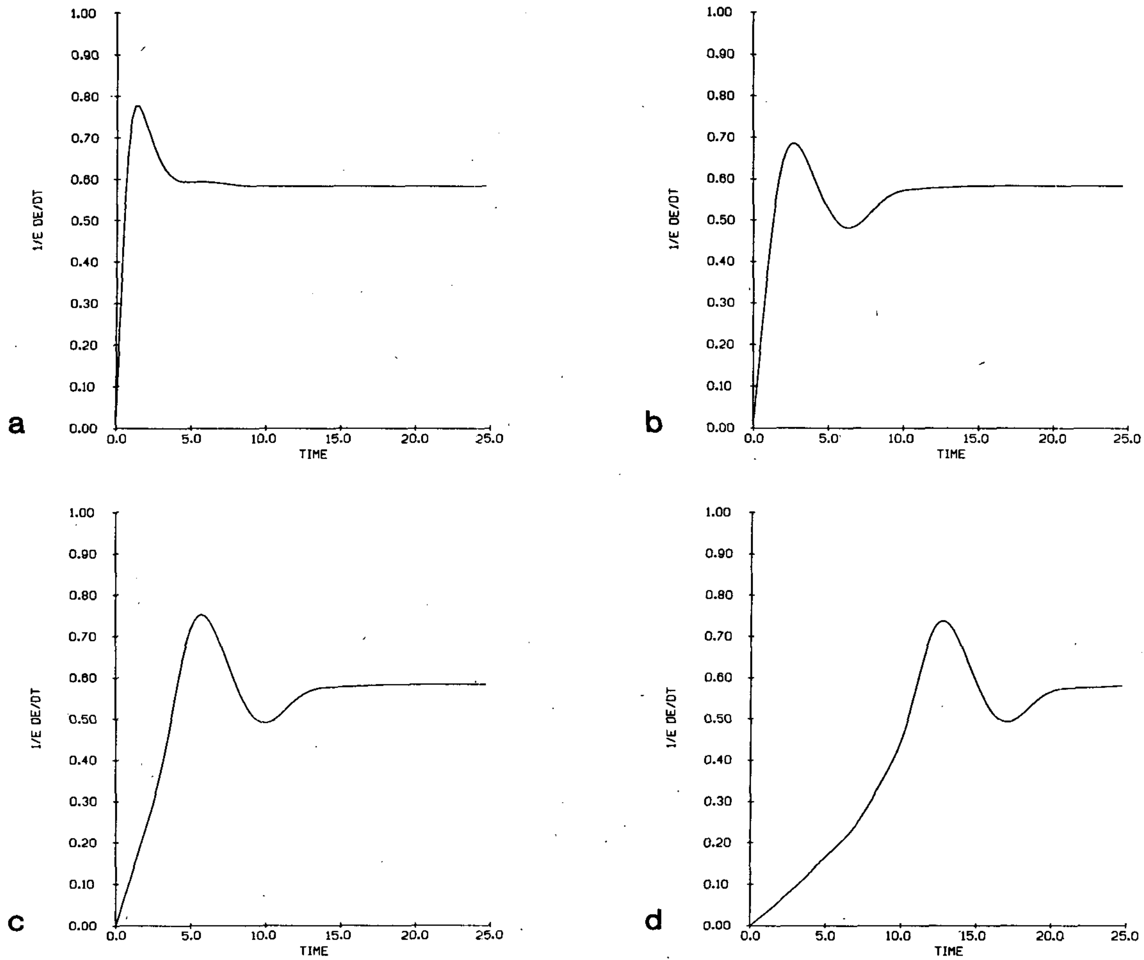

FIG. 11. The energy growth rate $2kc_{i_{eff}} = (1/E)(dE/dt)$ for the case in Fig. 10, with horizontal wavenumber $k_m = 1.8$ and perturbation vertical wavenumber $l = m\pi$. $m = 0, 2, 4, 8$ for (a), (b), (c) and (d), respectively.

ponentially unstable wave has an energy growth $E(t)/E(0) = e^{2kc_it}$, the results of initial value integrations for unstable waves will be displayed by plotting the instantaneous growth rate

$$2kc_{i_{eff}} = \frac{1}{E}\frac{dE}{dt}.$$

Integrations were performed for $k = k_m$ and initial perturbation vertical wavenumbers, $l = m\pi$, $m = 0$, 2, 4, 8. The growth rate as a function of time is shown in Fig. 4. Associated streamfunctions are also shown in Fig. 5. The region of neutral discrete normal modes at $k = 2.4$ yields the results in Figs. 6 and 7, and $k = 3.0$ yields the results in Figs. 8 and 9.

We are fortunate in the case of the Eady problem in that there exists a solution for arbitrary k and $m = 0$ in terms of a definite integral which is easily evaluated numerically (Simmons and Hoskins, 1979). Solutions generated for $m = 0$ by the matrix method described above were found to agree with this independent solution.

7. Discussion of Eady solutions

For orientation purposes some rules of thumb are noted first. The mechanism of initial value growth is similar to that described in the Couette problem, except for the reinterpretation of variables previously remarked on. The quantities ψ_x and ψ_z are initially in quadrature so the growth rate is zero at $t = 0$. As the perturbation is sheared by the mean flow, it acquires correlations and begins to extract energy from the mean flow. The time scale for this process is $\tau = l/k$, the ratio of the vertical to horizontal wavenumbers and the energy extracted increases with vertical wavenumber.

Comparing Figs. 4 and 6, the surprising result is found that for a wavenumber of 4 in the vertical initial perturbation and for times as large as $t = 5$, corresponding to much of the geophysically relevant

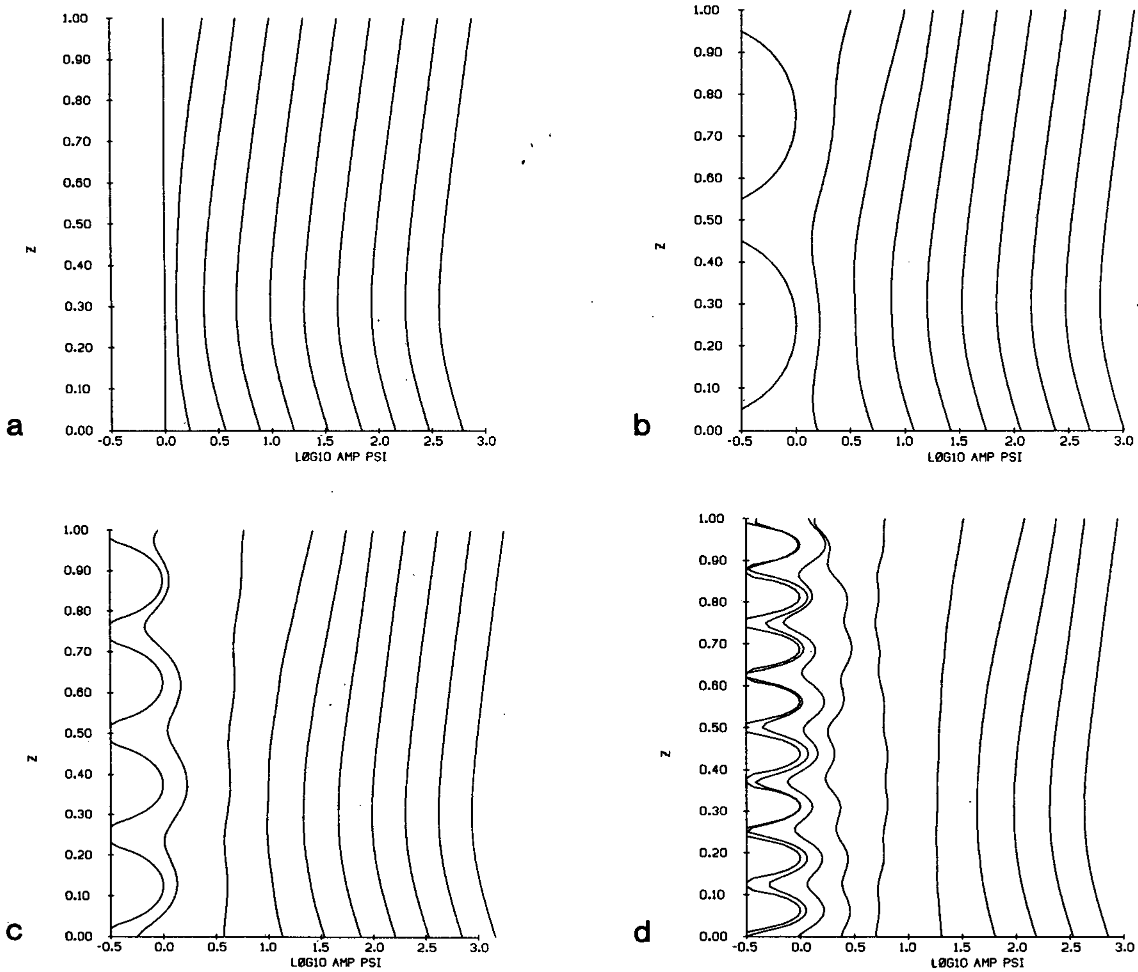

FIG. 12. Streamfunction amplitudes for the examples in Fig. 11. Samples are taken at $t = N\Delta t$, $N = 0, 1, 2 \cdots 9$, $\Delta t = 2.5$. Identification is direct, as surface values of $|\Psi|$ increase monotonically with time.

interval, the neutral wave at $k = 2.4$ grows as rapidly as the most unstable wave at $k_m = 1.6062$. This behavior persists down to vertical wavenumber 1, although over a somewhat shorter but not insignificant interval in time. It would seem, from the observation that neutral waves are able to grow in surface perturbation pressure by nearly three orders of magnitude and by a factor of 100 over a shorter time than the most rapidly growing exponential wavenumber, that more emphasis should be placed on the excitation of disturbances than has previously been the case.

The neutral waves at $k = 3.0$ (Figs. 8 and 9) extract large amounts of energy from the mean flow for large m and, being equally excited and nonorthogonal, undergo a vacillation cycle (Lindzen *et al.*, 1982) with a period given by

$$T = \frac{2\pi/k}{\Delta c}, \tag{28}$$

where Δc is the difference in normal mode phase speeds.

For $k = 3.0$ the normal modes have phase speeds of $c_1 = 0.66$ and $c_2 = 0.33$ resulting in a period from (28):

$$T = \frac{2\pi/3}{0.33} = 6.35,$$

as may be verified by examining Fig. 8. In Fig. 9, the streamfunction snapshots reveal the periodic vacillation in amplitude as the interference progresses. The region of dense samples should be viewed as an approximate envelope as the amplitude changes rapidly between samples.

8. The Green problem

A more realistic model results when the β-effect is included. To this end (20) is restricted to linear shear, $U(z) = z$, the β-plane approximation is made,

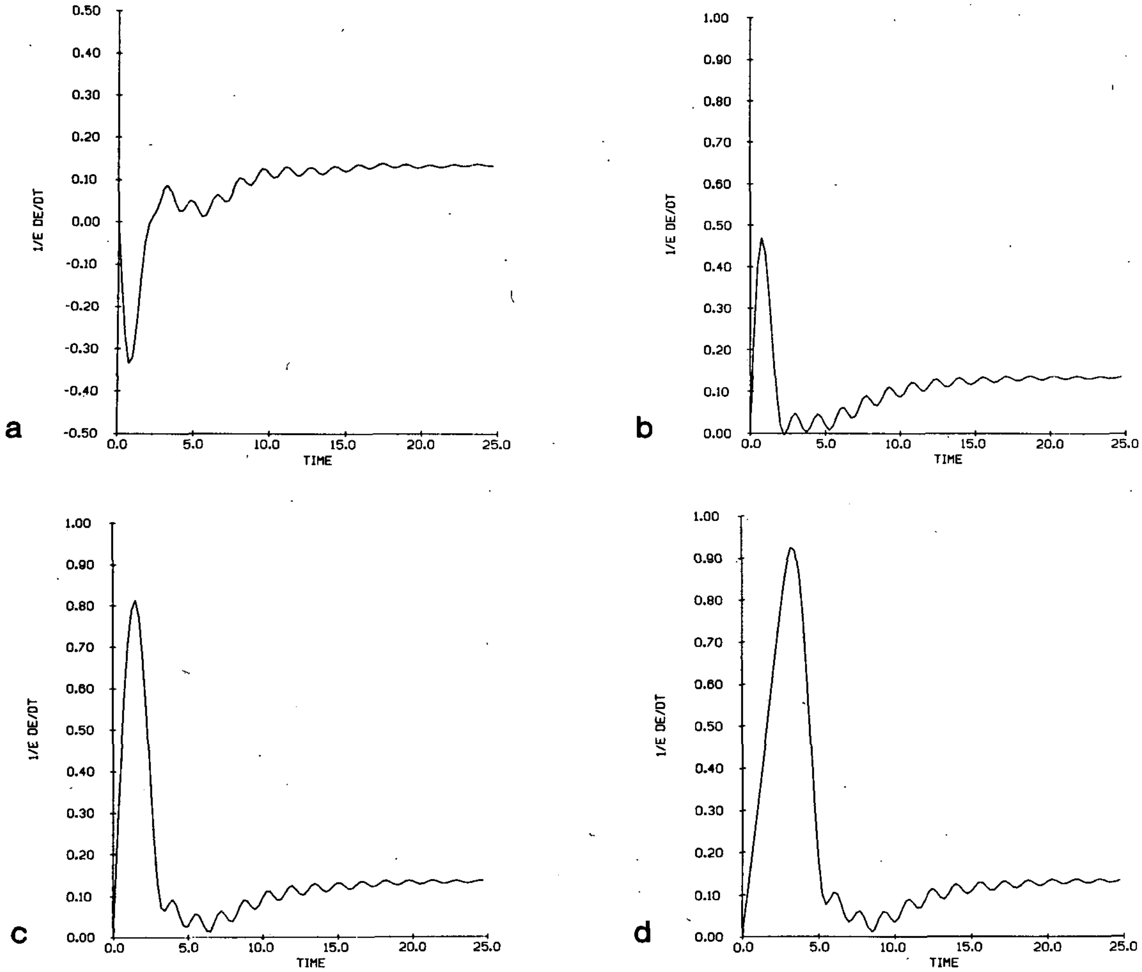

FIG. 13. As in Fig. 11, except for $k = 6.0$.

the Boussinesq approximation is made and rigid horizontal boundaries are imposed at $z = 0, H$. The nondimensional equation is (Lindzen *et al.*, 1980)

$$(z - c)\left(\frac{\partial^2}{\partial z^2} - k^2\right)\psi + r\psi = 0, \quad \text{(29a)}$$

$$(z - c)\psi_z - \psi = 0, \quad z = 0, 1, \quad \text{(29b)}$$

where the geostrophic streamfunction has been assumed to take the form

$$\Psi = \psi(z)e^{ik(x-ct)}$$

and

$$r = \frac{\beta H}{\epsilon \Lambda} \text{ stability parameter.}$$

This nondimensional equation has one stability parameter r, which for midlatitude scaling is

$$r = \frac{\beta H}{\epsilon \Lambda} = \frac{(1.6 \times 10^{-11}\ \mathrm{s^{-1}\ m^{-1}})(8 \times 10^3\ \mathrm{m})}{(1 \times 10^{-4})(1.25 \times 10^{-3}\ \mathrm{s^{-1}})} \approx 1.0.$$

With the choice $r = 1.0$, the eigenvalues of the discrete normal modes are as shown in Fig. 10a. There are two such modes at each value of k, an exponentially growing mode with the eigenvalue shown and a complex conjugate decaying mode not plotted in Fig. 10a. In addition, for $k < 1.3$ in the so-called Burger mode, there exists a third (neutral) normal mode with retrograde phase speed indicated by the dashed line in Fig. 10a.

Eigenmodes are shown in Fig. 10b for $k = 1.0$ and in Fig. 10c for $k_m = 1.8$ near the maximum exponential instability wavenumber and at $k = 6.0$.

Integrations were performed for $k = 1.8$ and initial perturbations of vertical wavenumber $l = m\pi$, $m = 0, 2, 4, 8$, with the results shown in Fig. 11. Streamfunction amplitudes are also shown (Fig. 12). In addition, results were obtained for $k = 6.0$ (Figs. 13 and 14).

The maximum exponential normal mode growth wavenumber $k_m = 1.8$ benefits marginally from the

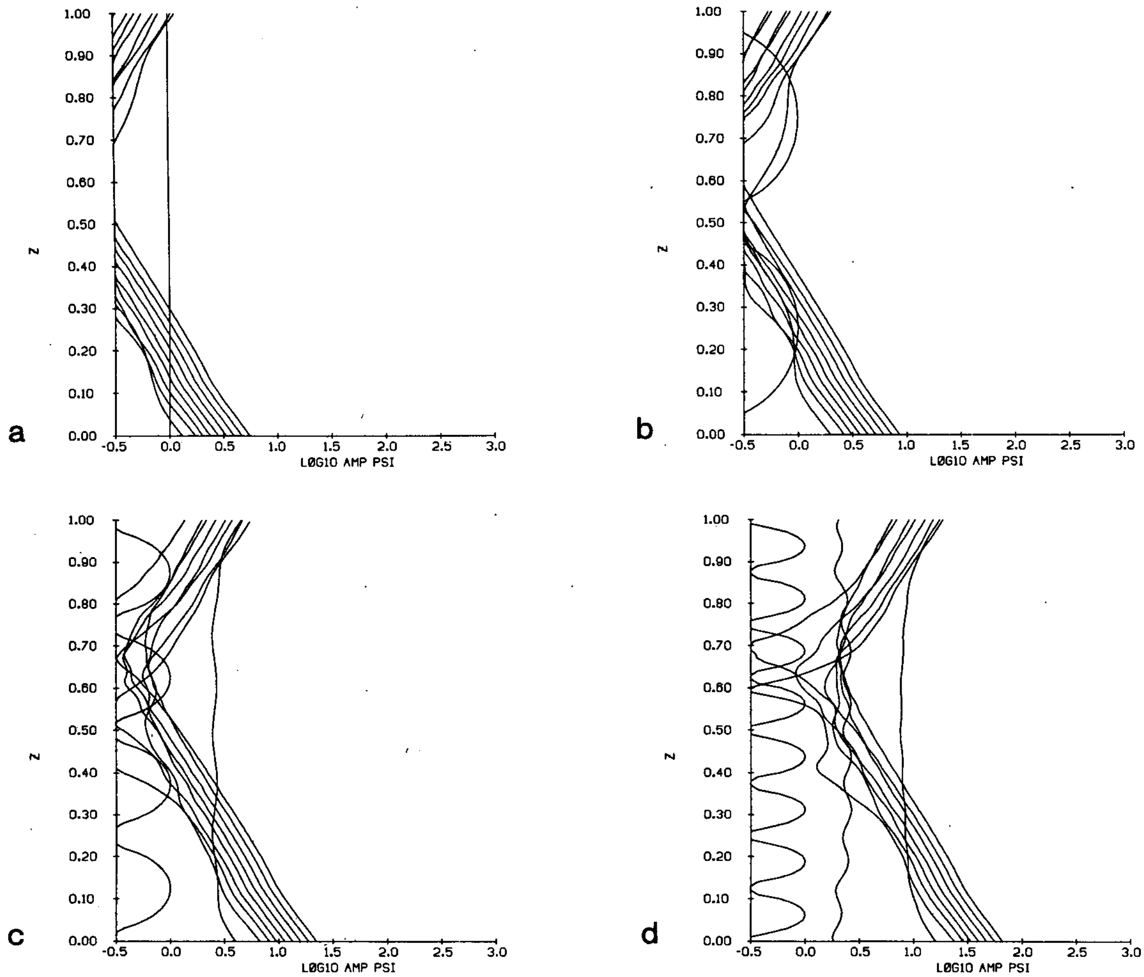

FIG. 14. As in Fig. 12, except for $k = 6.0$.

initial value growth and, in fact, is weakened out to $t = 10$ for $m = 4$, the correlations being set up slowly for this case (Figs. 11 and 12). The surprising result is the rapid initial growth of the $k = 6.0$ wave, for vertical wavenumber $l = m\pi$, $m = 2$ and $m = 4$ seen in Figs. 13 and 14. The very rapid initial setup of the short wavelength $k = 6.0$ mode suggests a role in cyclogenesis which will be discussed further in the sequel.

The case of Fig. 15 and Fig. 16 with $k = 1.0$ must be interpreted with caution as these long waves can be expected to penetrate many scale heights in the absence of an upper boundary, being the continuation of the neutral waves in the Charney problem (Charney, 1947).

The very small growth rates of the exponential normal modes for these long waves fail to dominate the solution until late in the development of the initial value problem, so that the normal mode growths may not be relevant to the excitation of the waves, a result that can be expected to persist in more realistic models. In addition the $m = 0$ example suggests that if the atmosphere supports retrograde neutral long waves of whatever origin, these will be excited in the initial value problem (say when the mean flow changes abruptly) and lead to vacillation with the slowly growing exponential modes (Lindzen *et al.*, 1982). The period for $k = 1.0$ with $c = -0.417, 0.285$ is, from (28)

$$T = \frac{2\pi/1.0}{0.285 + 0.417} = 8.95,$$

as may be verified by examination of Fig. 15.

The streamfunction magnitudes of Fig. 16 should be regarded as outlining an envelope with individual snapshots taken as the wave interference progresses.

As was noted above, the neutral retrograde normal mode also exists in the Charney problem and this was verified by removing the upper boundary to $Z_T = 16$ and imposing a radiation condition (Lindzen

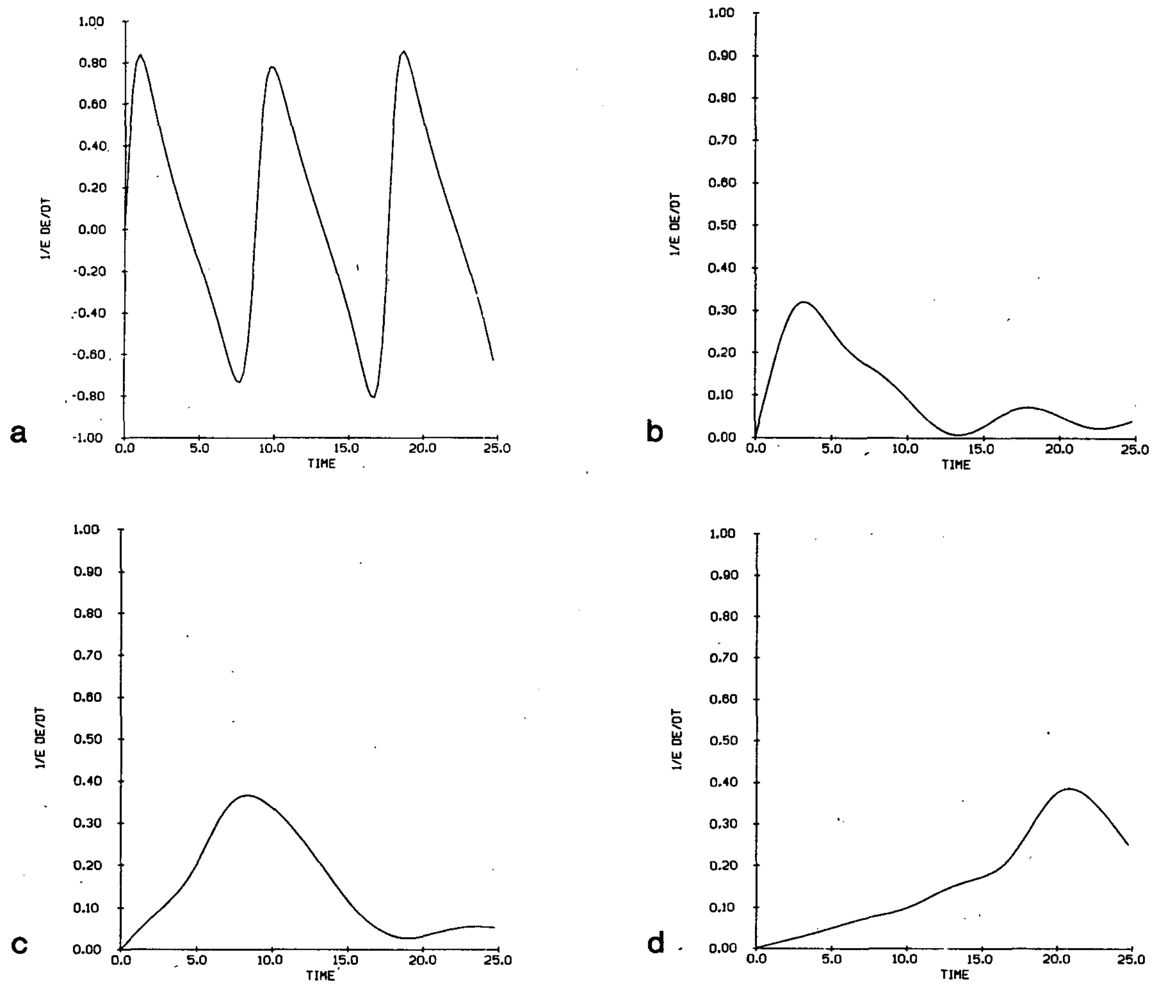

FIG. 15. As in Fig. 11, except for k = 1.0.

et al., 1980). It is identified as the extension of the neutral normal mode found by Burger (1962) and Miles (1964), and may be the analogue of the westerly waves seen in the atmosphere (Pratt and Wallace, 1976).

If the Boussinesq approximation is relaxed and the lid removed to great height, stratification enhances the effective growth in the stratosphere, so that a large response may develop from a small initial perturbation if the eigenfunctions involved have initially cancelling amplitudes in this region. A change in the mean zonal wind could lead to a large stratospheric response similar to the onset phase of sudden warmings. The fact that one of the modes responsible for the amplification is neutral, is of little consequence because the excitation results from initial value growth and, in fact, the exponentially unstable companion wave has such a small growth rate that it behaves as a neutral wave over relevant time scales.

Work to be reported elsewhere will more fully examine the phenomena outlined above.

9. An equilibrated flow

Recent work has focused attention on linearly equilibrated zonal flows (Stone, 1978; Lindzen *et al.*, 1980; Lindzen and Farrell, 1980). An example of such an equilibrated stationary solution is the above problem with the zonal velocity $u(z)$ modified to render $q_y \geq 0$ everywhere and $u = du/dz = 0$ at $z = 0$ (Lindzen and Farrell, 1980):

$$r - \frac{d^2u}{dz^2} = 0, \quad 0 \leq z < 1, \tag{30}$$

which has the solution for the above boundary conditions:

$$U(z) = \frac{r}{2} z^2, \tag{31}$$

which for r = 1.0 gives the stable to exponentially growing normal mode velocity profile

$$U(z) = \frac{z^2}{2}, \quad 0 \leq z \leq 1. \tag{32}$$

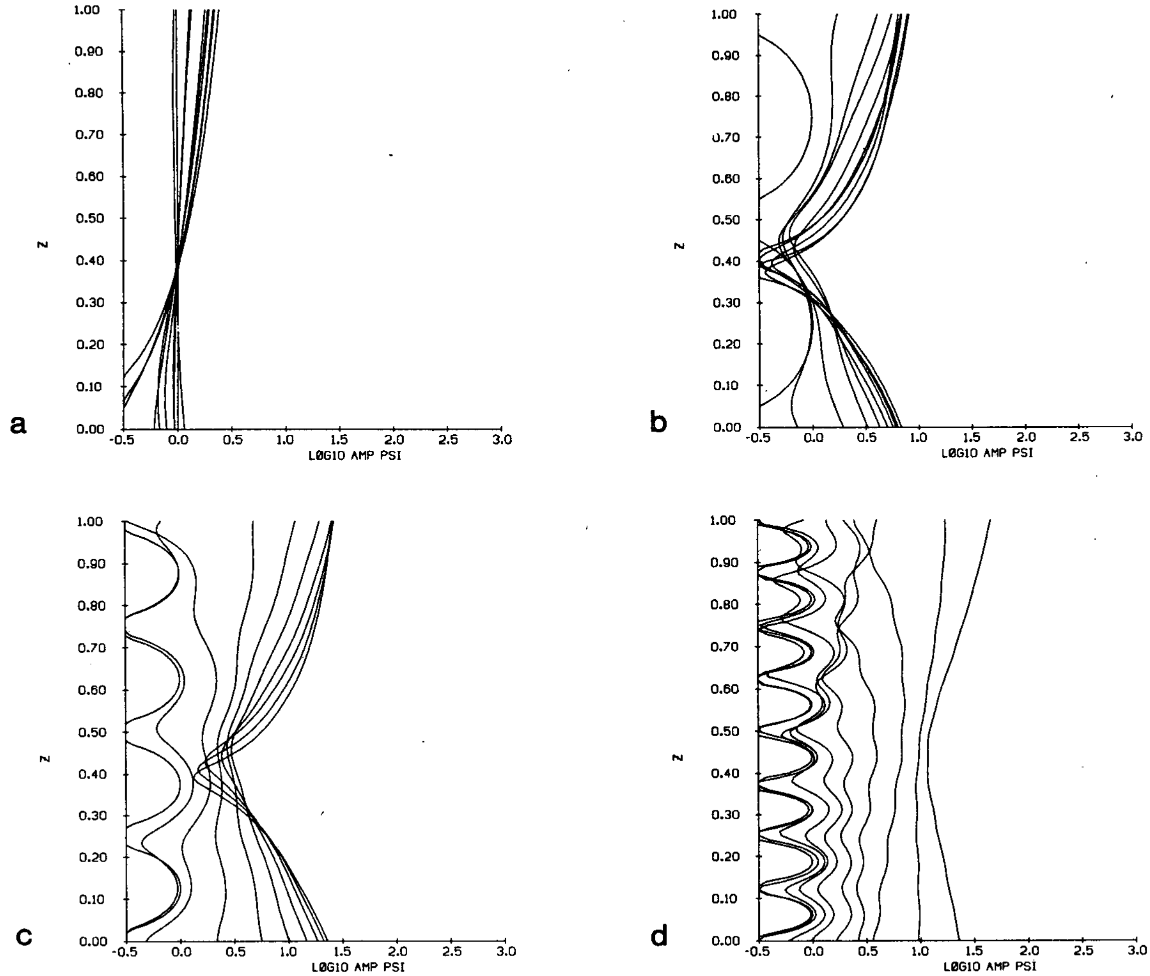

FIG. 16. As in Fig. 12, except for $k = 1.0$.

Integrations were performed for $k = 3.0$, and initial perturbation vertical wavenumbers $l = m\pi$, $m = 0, 2, 4, 8$. The growth rate as a function of time is shown in Fig. 17 with associated streamfunctions (Fig. 18).

At first glance, it may seem that with the potential vorticity of the mean equal to zero throughout the interior and at the lower boundary, that a severe restriction on growth of the kind detailed in Appendix A for the Couette problem could be imposed. However, there is a source of vorticity in the region of the upper boundary and examination of Fig. 18 shows that the high vertical wavenumber perturbation grows rapidly near this boundary, obtaining two-orders-of-magnitude amplification of perturbation pressure for $m = 4$.

Perturbations to this exponentially stabilized flow extract energy as an initial value problem and obtain maximum perturbation amplitude at the upper level in contrast to the Green normal mode (Fig. 14), which has its maximum at the lower boundary. We note that model studies (Simmons and Hoskins, 1978) have found similar behavior of disturbances in equilibrated mean flows. Although nonlinear effects are important in their work, the parallel is nonetheless suggestive.

The energy extracted from the mean is deposited asymptotically in two neutral waves with phase speeds $c_1 = 0$, and $c_2 = 0.165$, resulting in a vacillation as discussed previously with period from (28) of

$$T = \frac{2\pi/3.0}{0.165} = 12.7,$$

which may be verified by examination of Fig. 17.

It is remarkable that a phase-speed zero wave which supports no over-reflection (Lindzen *et al.*, 1980) obtains large amplitude in the initial value problem.

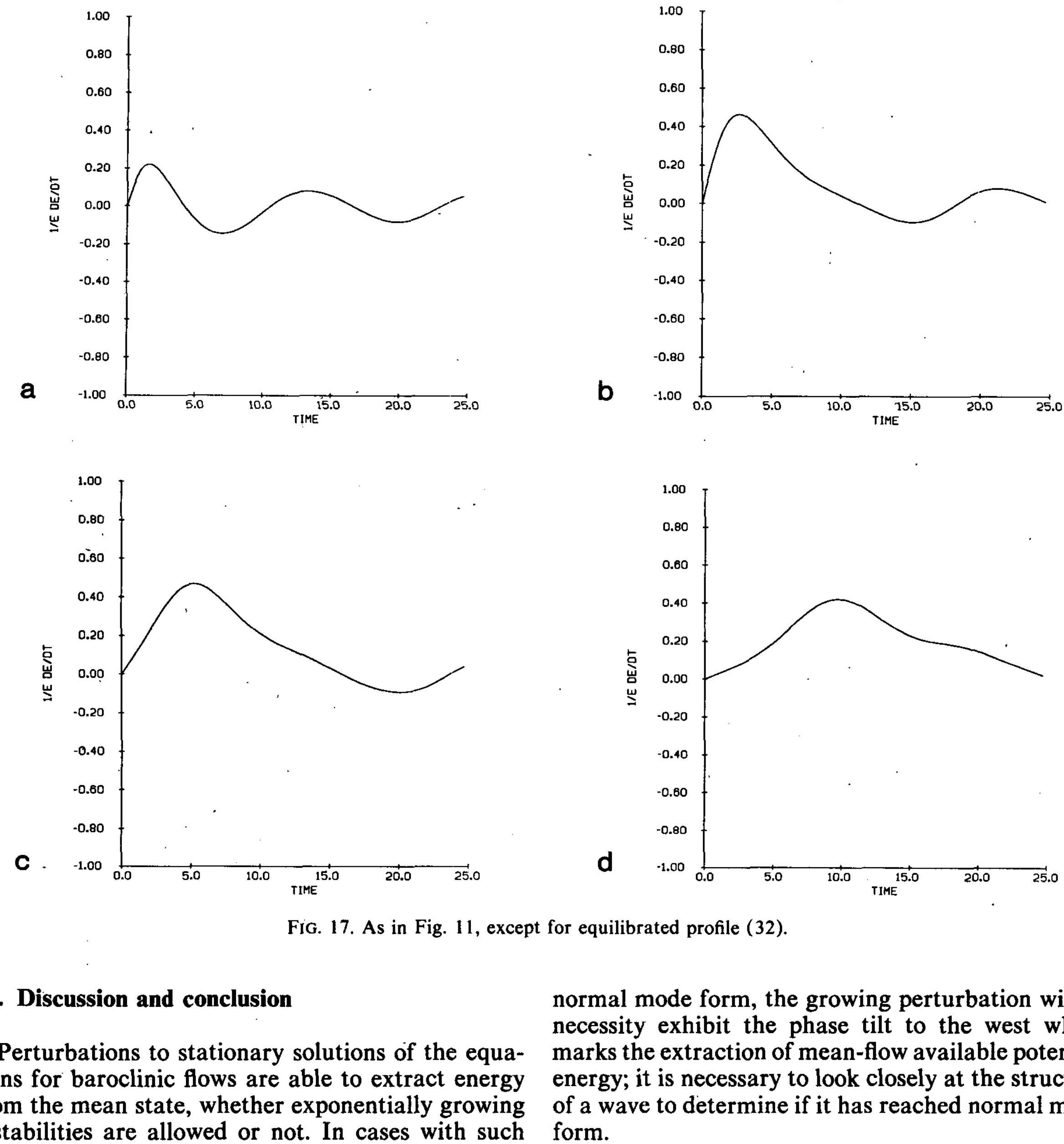

FIG. 17. As in Fig. 11, except for equilibrated profile (32).

10. Discussion and conclusion

Perturbations to stationary solutions of the equations for baroclinic flows are able to extract energy from the mean state, whether exponentially growing instabilities are allowed or not. In cases with such exponential modes, the degree to which the mode is excited is dependent on the initial condition so that the initial setup of the instability may proceed much more rapidly than would be predicted for the pure normal mode initial condition.

If cyclogenesis is initiated by a finite amplitude perturbation, the structure of the perturbation, in particular its vertical wavenumber, is crucial to the early stages of growth. The total amplification of a disturbance to a geophysical flow may be only a few e-foldings, say in going from a 2 mb depression to a 20 mb surface cyclone, in which case the growth may proceed to nonlinear equilibration without ever obtaining discrete normal mode form. While not of normal mode form, the growing perturbation will of necessity exhibit the phase tilt to the west which marks the extraction of mean-flow available potential energy; it is necessary to look closely at the structure of a wave to determine if it has reached normal mode form.

The time required for the exponentially unstable normal mode to dominate the solution depends on the vertical scale of the initial perturbation, being approximately $\tilde{t} = l/k$. For the $l = 4\pi$ examples this corresponds to nondimensional times of $\tilde{t} \sim 5$ and dimensional times from (27) of 1–4 days depending on the shear. Beyond this time the exponential modes dominate and the dynamics are described best using pulse asymptotic analysis (Simmons and Hoskins, 1979; Farrell, 1982).

A zonally localized initial condition can be expanded in a Fourier series in zonal wavenumber k. The magnitude of individual terms in this expansion is primarily determined by the initial conditions out

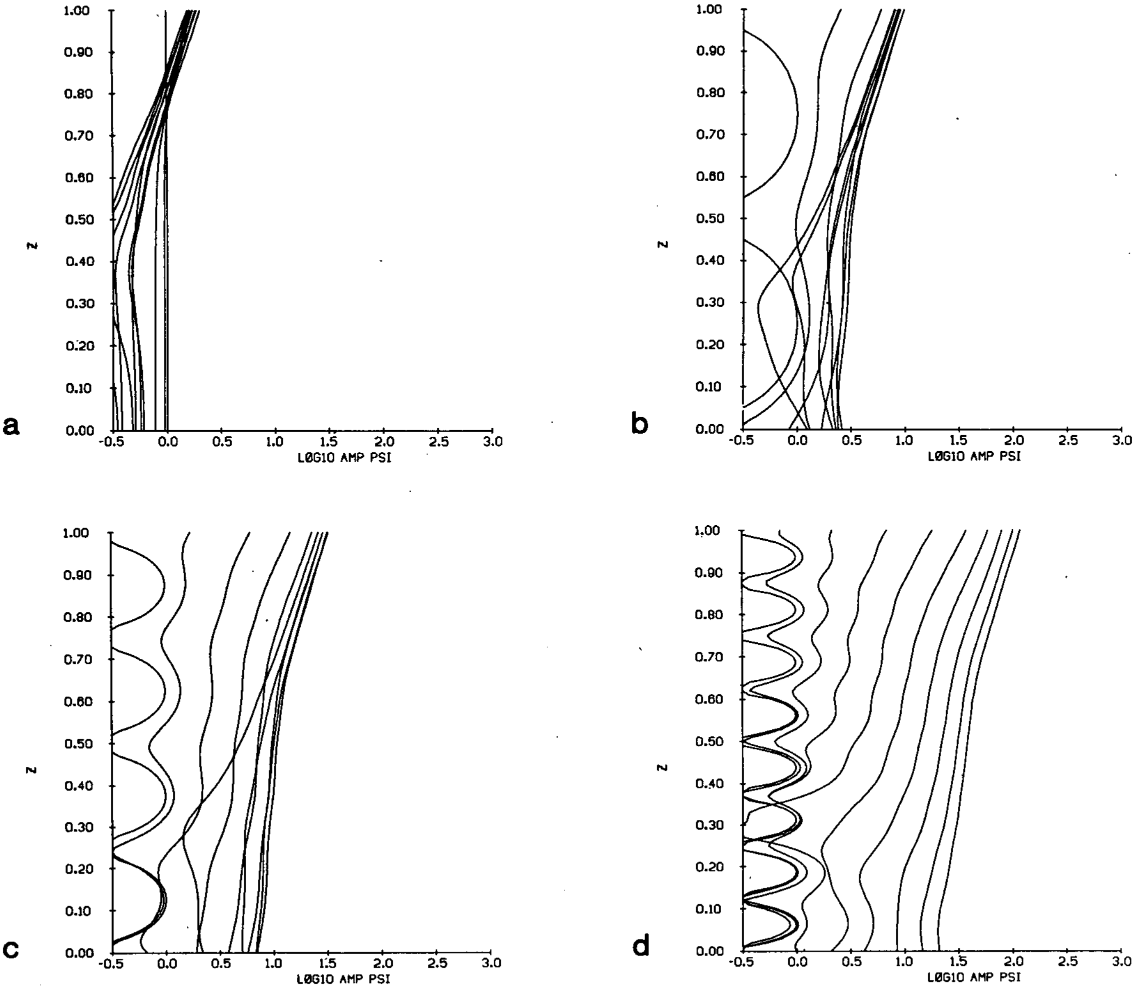

FIG. 18. As in Fig. 12, except for equilibrated profile (32).

to some time corresponding to a few days in dimensional time. It is at least plausible that the growth of the component perturbations will give rise to a similar growth of the localized pulse. This argument does not constitute a proof that the interference effects embodied in the Fourier composition will preserve the growth shown by individual wavenumbers. The evolution of a pulse and the effect of friction will be examined in future work.

In the case of stable flows, friction would eventually damp out the neutral normal modes excited by a perturbation or an impulsive spin up, and the continuous spectrum contribution would be expected to eventually decrease at least $O(t^2)$ as well. As it is common experimental practice to achieve a steady state and to decrease shocks to the system, the absence of persistent disturbances in annulus experiments, outside the range in parameter space where exponential instability is predicted, is not surprising. Interestingly, it is necessary to be very careful to reduce shocks in experiments exploring critical Reynolds number for transition to turbulence.

A baroclinic wave which causes the equilibration to exponential instability of a mean flow does not immediately lose the velocity/temperature correlations which result in the extraction of energy from the mean and will continue to grow. As shown in Section 9, the eigenfunctions, which are excited in initial value integrations for an equilibrated flow, have maximum amplitude and take energy from the mean at high levels in the model atmosphere, corresponding to the region where $\Pi_y > 0$. This contrasts with the eigenfunctions before equilibration which have maximum amplitude and extract energy at low levels.

If such equilibration of mean flows is as common an occurrence as has been recently argued (Lindzen and Farrell, 1980), then the secondary maxima of heat flux and wave amplitude in the upper troposphere seen both in observations and model experiments (Simmons and Hoskins, 1978) is to be expected.

If zero vertical wavenumber is effective in promoting growth of perturbations, then, as has been shown above, higher wavenumbers are even more effective. It is appropriate to ask if such complex vertical structure is found in the atmosphere.

It is unfortunate that observed profiles are usually extensively smoothed, obscuring the information on vertical structure; however, even in the smoothed data there is found evidence of large-scale coherent high wavenumber structure (Buzzi and Tibaldi, 1978, their Figs. 5 and 8; Hess and Wagner, 1948, their Figs. 7 and 8). Whether this structure serves as an initial condition in its own right or induces structure on a quasi-barotropic perturbation would be a subject for another investigation.

11. Application to cyclogenesis

It may be appropriate to indulge a speculation on rapid cyclogenesis. The energy growth curves discussed in Section 8 bear a striking resemblance to growth curves for initial stages of Alpine cyclogenesis (Buzzi and Tibaldi, 1978, their Fig. 12) and data for the initial stages of rapid cyclogenesis (Sanders and Gyakum, 1980). Pulse asymptotic theory can be expected to apply to these examples eventually and predicts the increase in horizontal scale noted as the waves consolidate into normal mode form late in the development (Simmons and Hoskins, 1979; Farrell, 1982). However, concentrating on the rapid first stage of growth, the fact that a sudden change in the wind velocity, whether from a trailing cold front (Buzzi and Tibaldi, 1978, their Fig. 1) or an advancing trough (Sanders and Gyakum, 1980; Hess and Wagner, 1948), is the immediate precursor of the cyclogenesis suggests that a forced stationary wave serves as the initial condition for the cyclogenesis. This mechanism agrees with the coincidence of regions of explosive cyclogenesis and mountains if we are willing to consider the Atlantic and Pacific western boundary currents as "thermal mountains." The waves would have to be of large horizontal extent $\lambda > 600$ km, which rules out pure gravity waves but agrees with observations of combined inertia-gravity waves (Hess and Wagner, 1948). Some interesting observations bearing on this proposed cyclogenic mechanism are contained in Chung *et al.* (1976).

The manner in which these waves would, in the course of collapsing, serve as initial perturbations for quasi-geostrophic baroclinic waves is subject for a model study.

Finally, we remark that if the growth of cyclone waves is dependent on the vertical structure of the initial condition to the extent found here, stringent requirements are implied for vertical resolution, both in observations and numerical simulations.

Acknowledgments. The author wishes to thank Dr. R. S. Lindzen for his helpful criticism, Dr. Arthur Rosenthal for kindly checking the approximations and lending his computer graphics expertise. This work was supported by NASA Grant NGL-22-007-228.

APPENDIX A

The basic state for the Couette problem possesses no vorticity and, in inviscid dynamics, there is no other source of vorticity except the initial perturbation. This fact may be exploited to obtain a bound on the initial value growth.

Consider an initial perturbation of horizontal wavenumber k and vertical wavenumber $m\pi$:

$$\psi = A_i \sin m\pi z \cos kx.$$

The energy from (15) is

$$E = \tfrac{1}{4}A_i^2[(m\pi)^2 + k^2]. \tag{A1}$$

The enstrophy is given by

$$\xi = \int_0^1 \tfrac{1}{2}(\bar{\psi}_{xx} + \bar{\psi}_{zz})^2 dz = \tfrac{1}{4}A_i^2[(m\pi)^4 + k^4]. \tag{A2}$$

As ξ is a constant for the flow, it must also be the enstrophy of the mode which maximizes E. The problem of maximizing E subject to the constraint that ξ be constant and the boundary conditions (1b) are met may be solved using the formalism of the variational calculus. For our purposes it is sufficient to note that maximum energy is associated with minimum vertical wavenumber and to choose the approximate maximum energy state as $m = 1$:

$$\psi_m = A_m \sin\pi z \cos kx.$$

If the initial perturbation has wavenumber $m\pi$ then the constancy of ξ requires from (A2):

$$\tfrac{1}{4}A_m^2(\pi^4 + k^4) = \tfrac{1}{4}A_i^2[(m\pi)^4 + k^4].$$

Hence the initial and approximate maximum amplitudes are related by

$$A_m^2 = A_i^2 \frac{(m\pi)^4 + k^4}{\pi^4 + k^4}.$$

The approximate maximum energy from (A1) is

$$E_m = A_i^2 \frac{(m\pi)^4 + k^4}{\pi^4 + k^4} \frac{\pi^2 + k^2}{4}.$$

The ratio of maximum to initial energy is

$$\frac{E_m}{E_i} = \left[\frac{(m\pi)^4 + k^4}{\pi^4 + k^4} \frac{\pi^2 + k^2}{4}\right]\left[\frac{(m\pi)^2 + k^2}{4}\right]^{-1}$$

$$= \frac{(m\pi)^4 + k^4}{(m\pi)^2 + k^2} \frac{\pi^2 + k^2}{\pi^4 + k^4}. \tag{A3}$$

The limit $k \to 0$ is

$$\frac{E_m}{E_i} = m^2, \qquad \text{(A4)}$$

whereas for $k = \pi$ near the maximum of growth rate we have

$$\frac{E_m}{E_i} = \frac{m^4 + 1}{m^2 + 1}, \qquad \text{(A5)}$$

which for $m \gg 1$ reduces to (A4). Comparing with Fig. 1a, a parallel behavior is seen and the perturbations fail to achieve these approximate maxima by only a small factor. For example as $k \to 0$, (14) reduces to

$$\lim_{k\to 0} \frac{E_m}{E_i} = \frac{(m\pi)^2}{24} \simeq 0.41\ m^2.$$

The above argument may be extended to the decay phase of the initial value problem for which conservation of enstrophy implies that the vertical wavenumber will increase linearly with time to give a t^{-2} decay in amplitude. Fig. 2b clearly shows this linear increase in wavenumber. Of course, it would be possible for a perturbation to decrease in amplitude by apportioning energy over many wavenumbers, so that this argument must be generalized to a Fourier sum (Charney, 1973).

APPENDIX B

With the substitution of (23), the linearized equation for the conservation of potential vorticity (20) can be written:

$$\left(\frac{\partial}{\partial t} + Uik\right)\left(-k^2 + \frac{\partial^2}{\partial z^2}\right)\psi(z, t) - \Pi_y ik\psi(z, t) = 0, \qquad \text{(B1a)}$$

$$\left(\frac{\partial}{\partial t} + Uik\right)\frac{\partial\psi(z, t)}{\partial z} - \frac{dU}{\partial z} ik\psi(z, t) = 0, \quad z = 0, 1. \qquad \text{(B1b)}$$

Forming the matrix operator $\nabla^2 = (-k^2 + \partial^2/\partial z^2)$ on $N + 2$ points by the usual finite difference approximation to derivatives and using (B1b) to eliminate the outlying boundary points allows (B1) to be written:

$$\frac{\partial}{\partial t} \nabla^2\psi = -ik[\mathbf{U}\nabla^2 - \mathbf{q}_y]\psi = 0.$$

$$\frac{\partial}{\partial t} \psi = -ik[\nabla^{2^{-1}}\mathbf{U}\nabla^2 - \nabla^{2^{-1}}\mathbf{q}_y]\psi.$$

Identifying $\mathbf{A} \equiv -ik[\nabla^{2^{-1}}\mathbf{U}\nabla^2 - \nabla^{2^{-1}}\mathbf{q}_y]$ results in a matrix eigenvalue problem for $\psi(z, t)$:

$$\frac{\partial}{\partial t} \psi = \mathbf{A}\psi. \qquad \text{(B2)}$$

If $\mathbf{A}$ has N distinct eigenvalues, λ_N then it has N associated linearly independent eigenvectors ψ_N. As the matrix $\mathbf{A}$ is not symmetric, these ψ_N are not in general orthogonal. The solution to (B2) for initial perturbation $\psi(z, 0)$ is

$$\psi(z, t) = \Lambda\mathbf{E}\Lambda^{-1}\psi(z, 0),$$

where

$$\Lambda = [\psi_1 \quad \psi_2 \cdots \psi_N],$$

the matrix of eigenvectors,

$$\mathbf{E} = \begin{bmatrix} e^{\lambda_1 t} & 0 \\ & \ddots \\ 0 & e^{\lambda_N t} \end{bmatrix},$$

the matrix of eigenvalue exponentials.

The solution as a function of time is, from (23):

$$\psi(x, z, t) = \psi(z, t)e^{ikx}.$$

With ∇^2 discretized using fourth-order differencing on $N = 100$ points, the QR algorithm requires less than 10 min to extract the eigenvectors using the modest DEC VAX 11/780 computer.

REFERENCES

Arnol'd, V. I., 1965: Conditions for nonlinear stability of stationary plane curvilinear flows of an ideal fluid. *Sov. Math. Dokl.*, **162,** 773–777.

Blumen, W., 1968: On the stability of quasi-geostrophic flow. *J. Atmos. Sci.*, **25,** 929–931.

Bretherton, F. P., 1966: Critical layer instability in baroclinic flows. *Quart. J. Roy. Meteor. Soc.*, **92,** 325–334.

Brown, S. N., and K. Stewartson, 1980: On the algebraic decay of disturbances in a stratified shear flow. *J. Fluid Mech.*, **100,** 811–816.

Burger, A. P., 1962: On the existence of critical wavelengths in a continuous baroclinic stability problem. *J. Atmos. Sci.*, **19,** 31–38.

——, 1966: Instability associated with the continuous spectrum in a baroclinic flow. *J. Atmos. Sci.*, **23,** 272–277.

Buzzi, A., and S. Tibaldi, 1978: Cyclogenesis in the lee of the Alps: a case study. *Quart. J. Roy. Meteor. Soc.*, **104,** 271–287.

Case, K. M., 1960: Stability of inviscid plane Couette flow. *Phys. Fluids*, **3,** 14.

——, 1961: Hydrodynamic stability and the inviscid limit. *J. Fluid Mech.*, **10,** 420–429.

Charney, J. G., 1947: The dynamics of long waves in a baroclinic westerly current. *J. Meteor.*, **4,** 135–162.

——, 1973: Planetary fluid dynamics. *Dynamic Meteorology*, P. Morel, Ed., D. Reidel, 97–351.

Chung, Y., K. Hage and E. Reinelt, 1976: On lee cyclogenesis and airflow in the Canadian Rocky Mountains and the East Asian Mountains. *Mon. Wea. Rev.*, **104,** 879–891.

Eady, E. J., 1949: Long waves and cyclone waves. *Tellus*, **1,** 33–52.

Hess, S. L., and H. Wagner, 1948: Atmospheric waves in the northwestern United States. *J. Meteor.*, **5,** 1–19.

Jeffreys, H., and B. Jeffreys, 1956: *Methods of Mathematical Physics*. Cambridge University Press, 718 pp.

Landahl, M. T., 1975: Wave breakdown and turbulence. *SIAM J. Appl. Math.*, **28,** 735–756.

Lin, C. C., 1961: Some mathematical problems in the theory of the stability of parallel flows. *J. Fluid Mech.*, **10,** 430–438.

Lindzen, R. S., and B. Farrell, 1980: The role of polar regions in global climate, and a new parameterization of global heat transport. *Mon. Wea. Rev.*, **108,** 2064–2079.

——, —— and K.-K. Tung, 1980: The concept of wave over-reflection and its application to baroclinic instability. *J. Atmos. Sci.*, **37,** 44–63.

——, —— and D. Jaqmin, 1982: Vacillations due to wave interference. Applications to the atmosphere and to annulus experiments. *J. Atmos. Sci.*, **39,** 14–23.

Miles, J. W., 1964: A note on Charney's model of zonal-wind instability. *J. Atmos. Sci.*, **21,** 451–452.

Orr, W. McF., 1907: Stability or instability of the steady motions of a perfect liquid. *Proc. Roy. Irish Acad.*, **27,** 9–69.

Pedlosky, J., 1964: An initial value problem in the theory of baroclinic instability. *Tellus*, **16,** 12–17.

——, 1970: Finite amplitude baroclinic waves. *J. Atmos. Sci.*, **27,** 15–30.

——, 1979: *Geophysical Fluid Dynamics*. Springer-Verlag, 624 pp.

Pratt, R. W., and J. M. Wallace, 1976: Zonal propagation characteristics of large-scale fluctuations in the midlatitude troposphere. *J. Atmos. Sci.*, **33,** 1184–1194.

Sanders, F., and J. Gyakum, 1980: Synoptic-dynamic climatology of the "bomb". *Mon. Wea. Rev.*, **108,** 1589–1606.

Simmons, A. J., and B. Hoskins, 1978: The life cycles of some nonlinear baroclinic waves. *J. Atmos. Sci.*, **25,** 414–432.

——, and ——, 1979: The downstream and upstream development of unstable baroclinic waves. *J. Atmos. Sci.*, **36,** 1239–1254.

Stone, P. H., 1978: Baroclinic adjustment. *J. Atmos. Sci.*, **35,** 561–571.

Wilkinson, J. H., 1965: *The Algebraic Eigenvalue Problem*. Clarendon Press, 662 pp.